

P-06-90

Forsmark site investigation

Groundwater flow measurements and SWIW test in borehole KFM08A

Erik Gustafsson, Rune Nordqvist, Pernilla Thur
Geosigma AB

September 2006

Svensk Kärnbränslehantering AB

Swedish Nuclear Fuel
and Waste Management Co
Box 5864

SE-102 40 Stockholm Sweden

Tel 08-459 84 00

+46 8 459 84 00

Fax 08-661 57 19

+46 8 661 57 19



ISSN 1651-4416

SKB P-06-90

Forsmark site investigation

Groundwater flow measurements and SWIW test in borehole KFM08A

Erik Gustafsson, Rune Nordqvist, Pernilla Thur
Geosigma AB

September 2006

Keywords: AP PF 400-05-092, Forsmark, Hydrogeology, Borehole, Groundwater, Flow, Tracer tests, Dilution probe, SWIW test.

This report concerns a study which was conducted for SKB. The conclusions and viewpoints presented in the report are those of the authors and do not necessarily coincide with those of the client.

A pdf version of this document can be downloaded from www.skb.se

Abstract

This report describes the performance, evaluation and interpretation of in-situ groundwater flow measurements and a single well injection withdrawal tracer test (SWIW test) at the Forsmark site. The objective of the activity was to determine the groundwater flow in selected fractures/fracture zones intersecting the cored borehole KFM08A. The objective was also to determine transport properties of fractures by means of a SWIW test in the borehole.

Groundwater flow measurements were carried out in two single fractures and in three fracture zones at borehole lengths ranging from 188.5 to 688.5 m (elevation –160 to –550 m). Hydraulic transmissivity ranged within $T = 1.1 \cdot 10^{-8}$ – $2.2 \cdot 10^{-6}$ m²/s. The results of the dilution measurements in borehole KFM08A show that the groundwater flow varies considerably, nevertheless the general trend is that flow rates and Darcy velocities decrease with depth. Flow rate ranged from 0.03 to 2.21 ml/min and Darcy velocity from $9.3 \cdot 10^{-10}$ to $8.0 \cdot 10^{-8}$ m/s ($8.0 \cdot 10^{-5}$ – $6.9 \cdot 10^{-3}$ m/d), which are in accordance with results from previously performed dilution measurements under natural gradient conditions at the Forsmark site.

The SWIW test was carried out in a fracture zone at a borehole length of c. 410 m with a hydraulic transmissivity of $T = 1.1 \cdot 10^{-8}$ m²/s. The model evaluation was made using a radial flow model with advection, dispersion and linear equilibrium sorption as transport processes.

A result from the SWIW test is that there is a clear retardation/sorption effect of both cesium and rubidium. The value of the retardation factor R is for cesium about 34 and for rubidium about 21. Estimated tracer recovery at the last sampling time yields approximately 81%, 50% and 42% for Uranine, cesium and rubidium, respectively. The model simulations were carried out for four different values of porosity; 0.005, 0.01, 0.02, 0.05 (assuming a 0.1 m thick transport zone), resulting in estimates of longitudinal dispersivity within the range of 0.09–0.33 m.

Sammanfattning

Denna rapport beskriver genomförandet, utvärderingen samt tolkningen av in-situ grundvattenflödesmätningar och enhållspårförsök (SWIW test) i Forsmark. Syftet med aktiviteten var dels att bestämma grundvattenflödet i enskilda sprickor och sprickzoner som skär borrhålet KFM08A samt att bestämma transportegenskaper i potentiella flödesvägar genom att utföra och utvärdera SWIW test i borrhålet.

Grundvattenflödesmätningar genomfördes i två enskilda sprickor och i tre sprickzoner på nivåer från 188.5 till 688.5 m borrhålslängd (160 till 550 m under havsytan). Den hydrauliska transmissiviteten varierade inom intervallet $T = 1.1 \cdot 10^{-8} - 2.2 \cdot 10^{-6} \text{ m}^2/\text{s}$. Resultaten från utspädningsmätningarna i borrhål KFM08A visar att grundvattenflödet varierar avsevärt under naturliga, dvs ostörda hydrauliska förhållanden. Den generella trenden är dock att flödet och Darcy hastigheten minskar med djupet. Beräknade grundvattenflöden låg inom intervallet 0.03–2.21 ml/min och Darcy hastigheter från $9.3 \cdot 10^{-10}$ till $8.0 \cdot 10^{-8} \text{ m/s}$ ($8.0 \cdot 10^{-5} - 6.9 \cdot 10^{-3} \text{ m/d}$) beräknades. Resultaten överensstämmer med tidigare genomförda mätningar i Forsmark.

SWIW testet genomfördes i en sprickzon vid ca 410 m borrhålslängd med den hydrauliska transmissiviteten $T = 1.1 \cdot 10^{-8} \text{ m}^2/\text{s}$. Utvärderingen genomfördes med en radiell flödesmodell med advektion, dispersion och linjär jämviktssorption som transportprocesser.

SWIW testet visar en klar effekt av fördröjning/sorption av både cesium och rubidium. Retardationsfaktorn R är ca 34 för cesium och ca 21 för rubidium. Den beräknade återhämtningen av spårämnena i återpumpningsfasen var cirka 81 %, 50 % och 42 % för Uranin, cesium och rubidium. Modellpassningar till mätdata gjordes för fyra olika värden på porositet; 0.005, 0.01, 0.02 och 0.05 (antagande en 0.1 m bred transportzon), vilket resulterade i beräknad longitudinell dispersivitet från 0.09 till 0.33 m.

Contents

1	Introduction	7
2	Objective and scope	9
3	Equipment	11
3.1	Borehole dilution probe	11
3.1.1	Measurement range and accuracy	11
3.2	SWIW test equipment	13
3.2.1	Measurement range and accuracy	13
4	Execution	15
4.1	Preparations	15
4.2	Procedure	15
4.2.1	Groundwater flow measurement	15
4.2.2	SWIW tests	16
4.3	Data handling	16
4.4	Analyses and interpretation	16
4.4.1	The dilution method – general principles	16
4.4.2	The dilution method – evaluation and analysis	19
4.4.3	SWIW test – basic outline	19
4.4.4	SWIW test – evaluation and analysis	20
4.5	Nonconformities	21
5	Results	23
5.1	Dilution measurements	23
5.1.1	KFM08A, section 188.5–191.5 m	25
5.1.2	KFM08A, section 274.5–277.5 m	27
5.1.3	KFM08A, section 410.5–413.5 m	28
5.1.4	KFM08A, section 479.0–482.0 m	30
5.1.5	KFM08A, section 685.5–688.5 m	31
5.1.6	Summary of dilution results	33
5.2	SWIW test	37
5.2.1	Treatment of experimental data	37
5.2.2	Tracer recovery breakthrough in KFM08A, 410.5–413.5 m	37
5.2.3	Model evaluation KFM08, 410.5–413.5 m	41
6	Discussion and conclusions	47
7	References	51
Appendix A	Borehole data KFM08A	53
Appendix B1	Dilution measurement KFM08A 188.5–191.5 m	55
Appendix B2	Dilution measurement KFM08A 274.5–277.5 m	58
Appendix B3	Dilution measurement KFM01A 410.5–413.5 m	61
Appendix B4	Dilution measurement KFM02A 479.0–482.0 m	64
Appendix B5	Dilution measurement KFM02A 685.5–688.5 m	67
Appendix C	BIPS logging KFM08A	71

1 Introduction

SKB is currently conducting a site investigation for a deep repository in Forsmark, according to general and site specific programmes /SKB 2001ab/. Two, among several methods for site characterisation are in-situ groundwater flow measurements and single well injection withdrawal tests (SWIW tests).

This document reports the results gained by a SWIW test and groundwater flow measurements with the borehole dilution probe in borehole KFM08A. The work was conducted by Geosigma AB and carried out between November 2005 and January 2006 according to activity plan AP PF 400-05-092. In Table 1-1 controlling documents for performing this activity are listed. Both activity plans and method descriptions/instructions are SKB's internal controlling documents. Data and results were delivered to the SKB site characterization database SICADA.

The borehole KFM08A is situated near the inlet channel for the Forsmark nuclear power plants, Figure 1-1. KFM08A is a core borehole with an inclination of -60.89° from the horizontal plane at the top of the borehole. The borehole is in total 1,001 m long and cased down to 102 m. From 102 m down to 1,001 m the diameter is 77 mm.

Detailed information about borehole KFM08A is listed in Appendix A (excerpt from the SKB database SICADA).

Table 1-1. Controlling documents for performance of the activity.

Activity plan	Number	Version
Grundvattenflödesmätningar och SWIW-tester KFM08A	AP PF 400-05-092	1.0
Method documents	Number	Version
Metodbeskrivning för grundvattenflödesmätning	SKB MD 350.001	1.0
Kalibrering av tryckgivare, temperaturgivare och flödesmätare	SKB MD 353.014	2.0
Kalibrering av fluorescensmätning	SKB MD 353.015	2.0
Kalibrering Elektrisk konduktivitet	SKB MD 353.017	2.0
Utspädningsmätning	SKB MD 353.025	2.0
Löpande och avhjälpande underhåll av Utspädningssond	SKB MD 353.065	1.0
Systemöversikt – SWIW-test utrustning	SKB MD 353.069	1.0
Löpande och avhjälpande underhåll av SWIW-test utrustning	SKB MD 353.070	1.0
Kalibrering av flödesmätare i SWIW-test utrustning	SKB MD 353.090	1.0
Instruktion för rengöring av borrhålsutrustning och viss markbaserad utrustning	SKB MD 600.004	1.0
Instruktion för längdkalibrering vid undersökningar i kärnborrhål	SKB MD 620.010	1.0

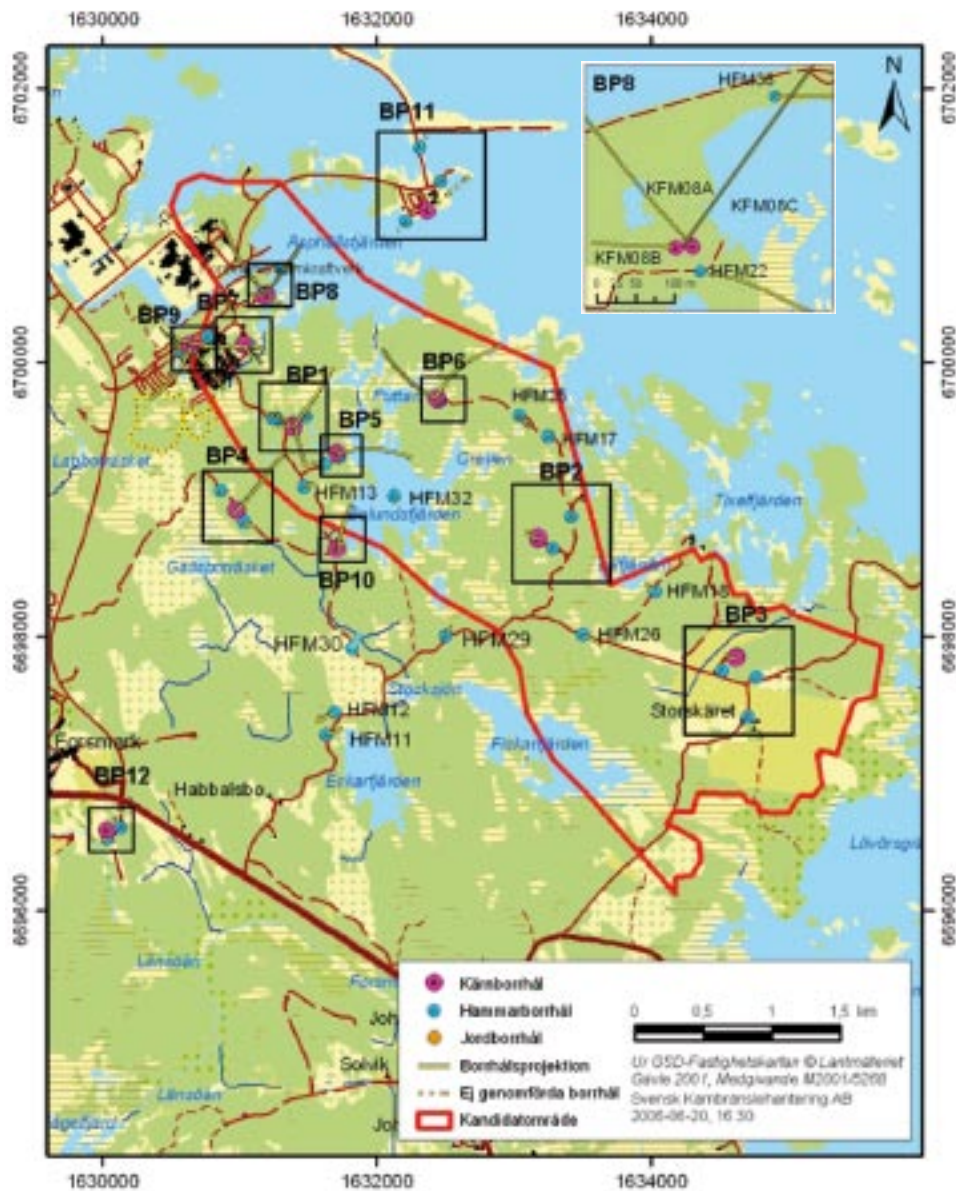


Figure 1-1. Overview of the Forsmark site investigation area, showing core boreholes (purple) and percussion boreholes (blue). A close-up of Drill Site 8 with KFM08A is shown in the upper right corner.

2 Objective and scope

The objective of the activity was to measure groundwater flow under a natural gradient in order to achieve information about natural flows and hydraulic gradients in the Forsmark area.

The objective of the SWIW test was to determine transport properties of groundwater flow paths in fractures/fracture zones in a depth range of 300–700 m and a hydraulic transmissivity of $1 \cdot 10^{-8}$ – $1 \cdot 10^{-6}$ m²/s in the test section.

The groundwater flow measurements were performed in fractures and fracture zones at a borehole length range of 188–685 m using the SKB borehole dilution probe. The hydraulic transmissivity in the test sections ranged between $1.1 \cdot 10^{-8}$ – $2.2 \cdot 10^{-6}$ m²/s. Groundwater flow measurements were performed in totally five test sections. In one of these sections a SWIW test was also performed, simultaneously using both sorbing and non-sorbing tracers.

3 Equipment

3.1 Borehole dilution probe

The borehole dilution probe is a mobile system for groundwater flow measurements, Figure 3-1. Measurements can be made in boreholes with 56 mm or 77 mm diameter and the test section length can be arranged for 1, 2, 3, 4 or 5 m with an optimised special packer/dummy system and section length between 1 and 10 m with standard packers. The maximum measurement depth is at 1,030 m borehole length. The vital part of the equipment is the probe which measures the tracer concentration in the test section down hole and in-situ. The probe is equipped with two different measurement devices. One is the Optic device, which is a combined fluorometer and light-transmission meter. Several fluorescent and light absorbing tracers can be used with this device. The other device is the Electrical Conductivity device, which measures the electrical conductivity of the water and is used for detection/analysis of saline tracers. The probe and the packers that straddle the test section are lowered down the borehole with an umbilical hose. The hose contains a tube for hydraulic inflation/deflation of the packers and electrical wires for power supply and communication/data transfer. Besides tracer dilution detection, the absolute pressure and temperature are measured. The absolute pressure is measured during the process of dilution because a change in pressure indicates that the hydraulic gradient, and thus the groundwater flow, may have changed. The pressure gauge and the temperature gauge are both positioned in the dilution probe, about seven metres from top of test section. This bias is not corrected for as only changes and trends relative to the start value are of great importance for the dilution measurement. Since the dilution method requires homogenous distribution of the tracer in the test section, a circulation pump is also installed and circulation flow rate measured.

A caliper log, attached to the dilution probe, is used to position the probe and test section at the pre-selected borehole length. The caliper detects reference marks previously made by a drill bit at exact length along the borehole, approximately every 50 m. This method makes it possible to position the test section with an accuracy of $c. \pm 0.10$ m.

3.1.1 Measurement range and accuracy

The lower limit of groundwater flow measurement is set by the dilution caused by molecular diffusion of the tracer into the fractured/porous aquifer, relative to the dilution of the tracer due to advective groundwater flow through the test section. In a normally fractured granite, the lower limit of a groundwater flow measurement is approximately at a hydraulic conductivity, K , between $6 \cdot 10^{-9}$ and $4 \cdot 10^{-8}$ m/s, if the hydraulic gradient, I , is 0.01. This corresponds to a groundwater flux (Darcy velocity), v , in the range of $6 \cdot 10^{-11}$ to $4 \cdot 10^{-10}$ m/s, which in turn may be transformed into groundwater flow rates, Q_w , corresponding to 0.03–0.2 ml/hour through a one m test section in a 76 mm diameter borehole. In a fracture zone with high porosity, and thus a higher rate of molecular diffusion from the test section into the fractures, the lower limit is about $K = 4 \cdot 10^{-7}$ m/s if $I = 0.01$. The corresponding flux value is in this case $v = 4 \cdot 10^{-9}$ m/s and flow rate $Q_w = 2.2$ ml/hour. The lower limit of flow measurements is, however, in most cases constrained by the time available for the dilution test. The required time frame for an accurate flow determination from a dilution test is within 7–60 hours at hydraulic conductivity values greater than about $1 \cdot 10^{-7}$ m/s. At conductivity values below $1 \cdot 10^{-8}$ m/s, measurement times should be at least 70 hours for natural (undisturbed) hydraulic gradient conditions.

The upper limit of groundwater flow measurements is determined by the capability of maintaining a homogeneous mix of tracer in the borehole test section. This limit is determined by several factors, such as length of the test section, volume, distribution of the water conducting fractures and how the circulation pump inlet and outlet are designed. The practical upper measurement limit is about 2,000 ml/hour for the equipment developed by SKB.

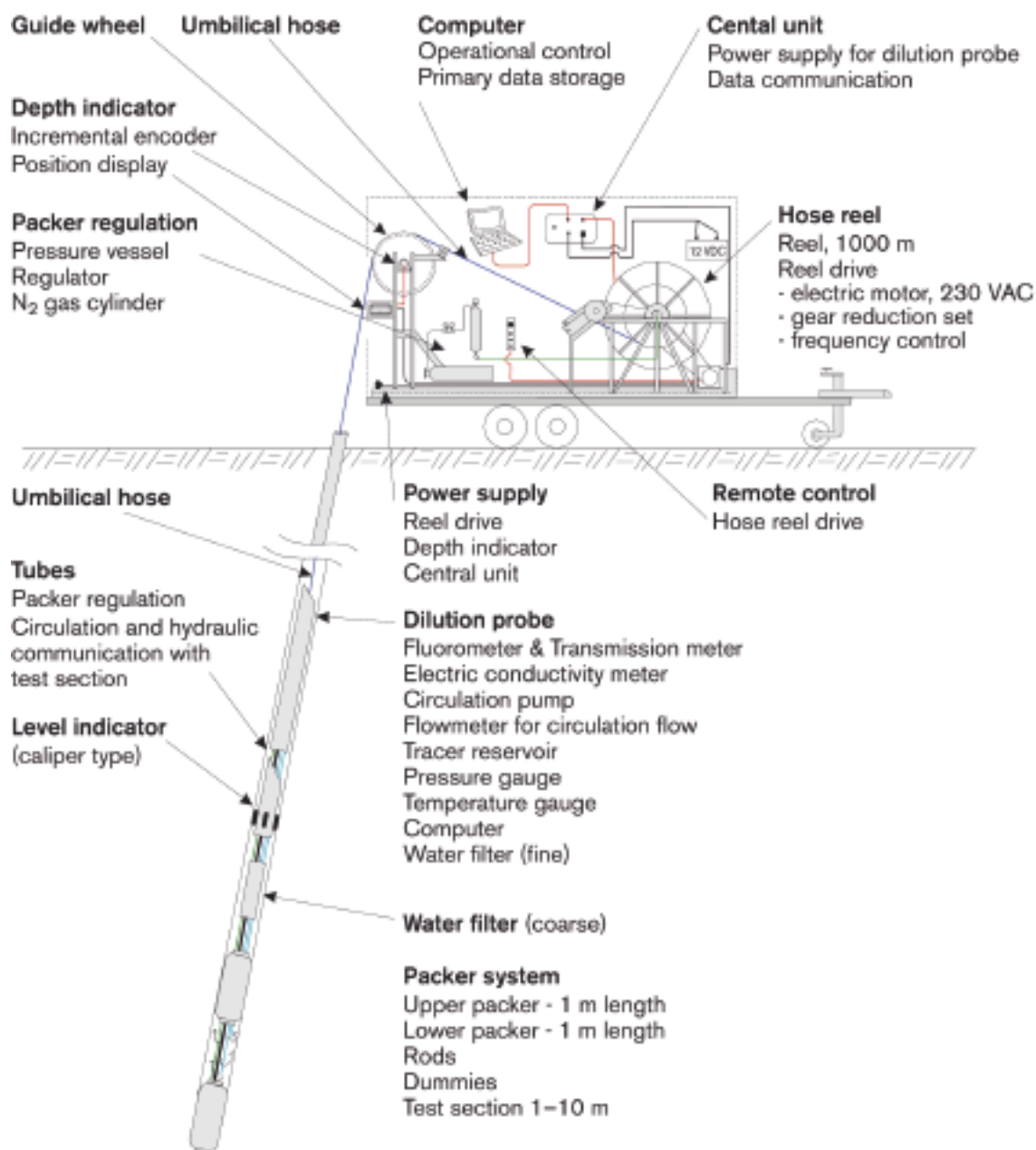


Figure 3-1. The SKB borehole dilution probe.

The accuracy of determined flow rates through the borehole test section is affected by various measurement errors related to, for example, the accuracy of the calculated test section volume and determination of tracer concentration. The overall accuracy when determining flow rates through the borehole test section is better than $\pm 30\%$, based on laboratory measurements in artificial borehole test sections.

The groundwater flow rates in the rock formation are determined from the calculated groundwater flow rates through the borehole test section and by using some assumption about the flow field around the borehole test section. This flow field depends on the hydraulic properties close to the borehole and is given by the correction factor α , as discussed below in Section 4.4.1. The value of α will, at least, vary within $\alpha = 2 \pm 1.5$ in fractured rock /Gustafsson 2002/. Hence, the groundwater flow in the rock formation is calculated with an accuracy of about $\pm 75\%$, depending on the flow-field distortion.

3.2 SWIW test equipment

The SWIW (Single Well Injection Withdrawal) test equipment constitutes a complement to the borehole dilution probe making it possible to carry out a SWIW test in the same test section as the dilution measurement, Figure 3-2. Measurements can be made in boreholes with 56 mm or 77 mm diameter and the test section length can be arranged for 1, 2, 3, 4 or 5 m with an optimised special packer/dummy system for 76 mm boreholes. The equipment is primarily designed for measurements in the depth interval 300–700 m borehole length. However, measurements can be carried out at shallower depths as well at depths larger than 700 m. The possibility to carry out a SWIW test much depends on the hydraulic transmissivity in the investigated test section and frictional loss in the tubing at tracer withdrawal pumping. Besides the dilution probe, the main parts of the SWIW test equipment are:

- Polyamide tubing constituting the hydraulic connection between SWIW test equipment at ground surface and the dilution probe in the borehole.
- Air tight vessel for storage of groundwater under anoxic conditions, i.e. N₂-atmosphere.
- Control system for injection of tracer solution and groundwater (chaser fluid).
- Injection pumps for tracer solution and groundwater.

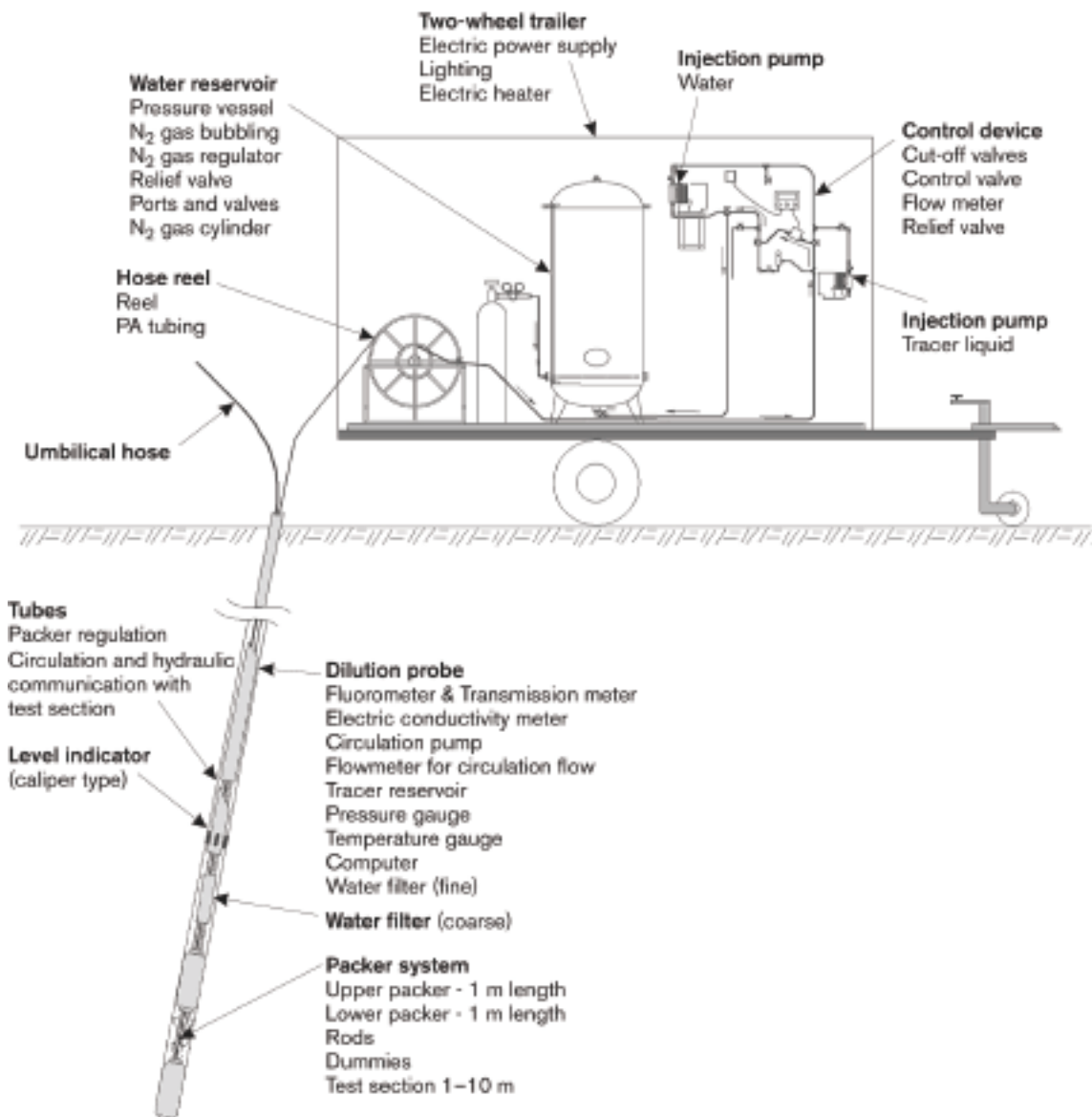


Figure 3-2. SWIW test equipment, connected to the borehole dilution probe.

The result of a SWIW test depends on the accuracy in the determination of the tracer concentration in injection solutions and withdrawn water. The result also depends on the accuracy in the volume of injection solution and volumes of injected and withdrawn water. For non-sorbing dye tracers (e.g. Uranine) the tracer concentration in collected water samples can be analysed with a resolution of 10 µg/l in the range 0.0–4.0 mg/l. The accuracy is within $\pm 5\%$. The volume injected tracer solution can be determined within $\pm 0.1\%$ and the volume of injected and withdrawn water determined within $\pm 5\%$.

The evaluation of a SWIW test and determination of transport parameters is done with model simulations, fitting the model to the measured data (concentration as a function of time). The accuracy in determined transport parameters depends on selection of model concept and how well the model fit the measured data.

4 Execution

The measurements were performed according to AP PF 400-05-092 (SKB internal controlling document) in compliance with the methodology descriptions for the borehole dilution probe equipment – SKB MD 350.001, Metodbeskrivning för grundvattenflödesmätning –, and the measurement system description for SWIW test – SKB MD 353.069, MSB; Systemöversikt – SWIW-test utrustning – (SKB Internal controlling documents), Table 1-1.

4.1 Preparations

Both the fluorometer and the electric conductivity meter were calibrated, according to SKB Internal controlling documents MD 353.015 and MD 353.017, before arriving at the site. Briefly, this was performed by adding certain amounts of the tracer to a known test volume while registering the measured A/D-levels. From this, calibration constants were calculated and saved for future use by using the measurement application. The other sensors had been calibrated previously (SKB MD 353.014 and 353.090) and were hence only control calibrated.

Extensive functionality checks were performed prior to transport to the site and limited function checks were performed at the site, according to SKB MD 353.065 and MD 353.070.

The equipment was cleaned to comply with SKB cleaning level 1 (SKB MD 600.004) before lowering it into the borehole.

4.2 Procedure

4.2.1 Groundwater flow measurement

In total five groundwater flow measurements were carried out, Table 4-1. Each measurement was performed according to the following procedure. The equipment was lowered to the correct borehole length where background values of tracer concentration and supporting parameters, pressure and temperature, were measured and logged. Then, after inflating the packers and the pressure had stabilized, tracer was injected in the test section. The tracer concentration and supporting parameters were measured and logged continuously until the tracer had been diluted to such a degree that the groundwater flow rate could be calculated. For a detailed description of how the measurement is performed see SKB MD 353.025.

Table 4-1. Performed dilution (flow) measurements.

Borehole	Test section (m)	Number of flowing fractures*	T (m ² /s)*	Tracer	Measurement period (yymmdd–yymmdd)
KFM08A	188.5–191.5	1	2.20E–06	Uranine	051111–051114
KFM08A	274.5–277.5	3–4	1.29E–06	Uranine	051114–051116
KFM08A	410.5–413.5	3	1.13E–08	Uranine	051209–051215
KFM08A	479.0–482.0	1–2	6.93E–08	Uranine	051121–051124
KFM08A	685.5–688.5	1	1.41E–06	Uranine	051116–051121

* /Sokolnicki and Rouhiainen 2005/.

4.2.2 SWIW tests

One SWIW test was performed, Table 4-2. To conduct a SWIW test requires that the SWIW equipment is connected to the borehole dilution probe, Figures 3-1 and 3-2.

The SWIW test was performed according to the following procedure. The equipment was lowered to the right borehole length where background values of Uranine and supporting parameters, pressure and temperature, were measured and logged. Then, after inflating the packers and the pressure had stabilized, the circulation pump in the dilution probe was used to pump groundwater from the test section to the air tight vessel at ground surface. Water samples were also taken for analysis of background concentration of Uranine, rubidium and cesium. When pressure had recovered after the pumping in the test section, the injection phases started with pre-injection of the native groundwater to reach steady state flow conditions. Thereafter groundwater spiked with the tracers Uranine, rubidium and cesium was injected. At last injection of native groundwater to push the tracers out into the fracture/fracture zone was performed. The withdrawal phase started by pumping water to the ground surface. An automatic sampler at ground surface was used to take water samples for analysis of Uranine, rubidium and cesium in the withdrawn water.

4.3 Data handling

During groundwater flow measurement with the dilution probe, data are automatically transferred from the measurement application to a SQL database. Data relevant for analysis and interpretation are then automatically transferred from SQL to Excel via an MSSQL (ODBC) data link, set up by the operator. After each measurement the Excel data file is copied to a CD.

The water samples from the SWIW test was analysed for Uranine tracer content at the Geosigma Laboratory in Uppsala. Cesium and rubidium content were analysed at the Analytica laboratory in Luleå.

4.4 Analyses and interpretation

4.4.1 The dilution method – general principles

The dilution method is an excellent tool for in-situ determination of flow rates in fractures and fracture zones.

In the dilution method a tracer is introduced and homogeneously distributed into a bore-hole test section. The tracer is subsequently diluted by the ambient groundwater, flowing through the borehole test section. The dilution of the tracer is proportional to the water flow through the borehole section, Figure 4-1.

Table 4-2. Performed SWIW tests.

Borehole	Test section (m)	Number of flowing fractures*	T (m ² /s)*	Tracers	Measurement period (yymmdd–yymmdd)
KFM08A	410.5–413.5	3	1.13E–08	Uranine/ cesium/ rubidium	051125–060103

* /Sokolnicki and Rouhiainen 2005/.

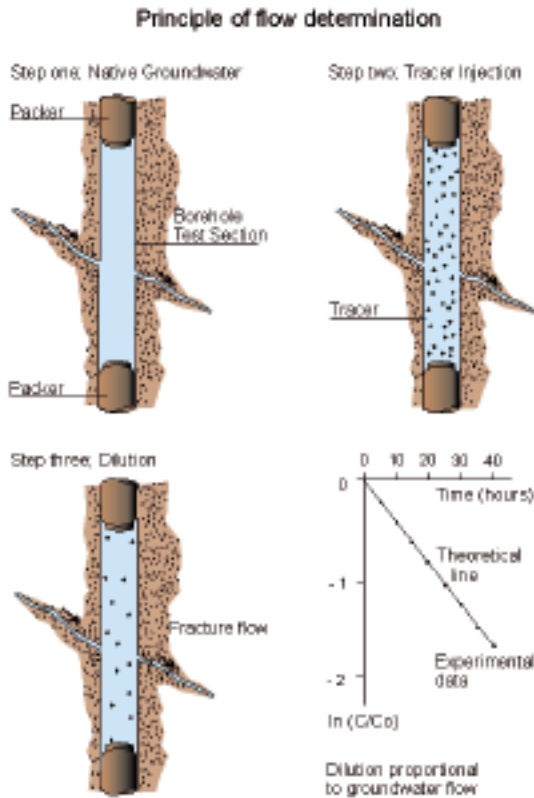


Figure 4-1. General principles of dilution and flow determination.

The dilution in a well-mixed borehole section, starting at time $t = 0$, is given by:

$$\ln(C/C_0) = -\frac{Q_w}{V} \cdot t \quad (\text{Equation 4-1})$$

where C is the concentration at time t (s), C_0 is the initial concentration, V is the water volume (m^3) in the test section and Q_w is the volumetric flow rate (m^3s^{-1}). Since V is known, the flow rate may then be determined from the slope of the line in a plot of $\ln(C/C_0)$, or $\ln C$, versus t .

An important interpretation issue is to relate the measured groundwater flow rate through the borehole test section to the rate of groundwater flow in the fracture/fracture zone straddled by the packers. The flow-field distortion must be taken into consideration, i.e. the degree to which the groundwater flow converges and diverges in the vicinity of the borehole test section. With a correction factor, α , which accounts for the distortion of the flow lines due to the presence of the borehole, it is possible to determine the cross-sectional area perpendicular to groundwater flow by:

$$A = 2 \cdot r \cdot L \cdot \alpha \quad (\text{Equation 4-2})$$

where A is the cross-sectional area (m^2) perpendicular to groundwater flow, r is borehole radius (m), L is the length (m) of the borehole test section and α is the correction factor. Figure 4-2 schematically shows the cross-sectional area, A , and how flow lines converge and diverge in the vicinity of the borehole test section.

Assuming laminar flow in a plane parallel fissure or a homogeneous porous medium, the correction factor α is calculated according to Equation (4-3), which often is called the formula of Ogilvi /Halevy et al. 1967/. Here it is assumed that the disturbed zone, created by the presence of the borehole, has an axis-symmetrical and circular form.

$$\alpha = \frac{4}{1 + (r/r_d) + (K_2/K_1) (1 - (r/r_d)^2)} \quad (\text{Equation 4-3})$$

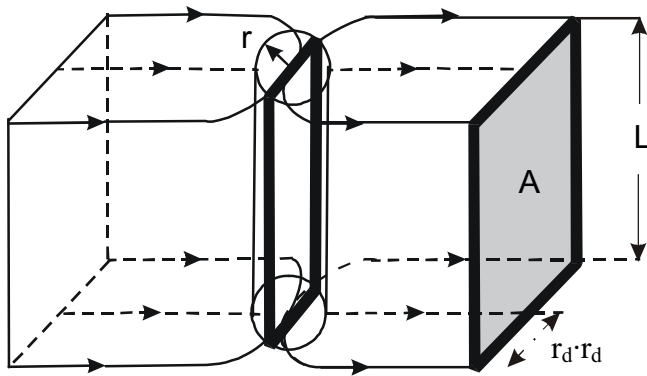


Figure 4-2. Diversion and conversion of flow lines in the vicinity of a borehole test section.

where r_d is the outer radius (m) of the disturbed zone, K_1 is the hydraulic conductivity (m/s) of the disturbed zone, and K_2 is the hydraulic conductivity of the aquifer. If the drilling has not caused any disturbances outside the borehole radius, then $K_1 = K_2$ and $r_d = r$ which will result in $\alpha = 2$. With $\alpha = 2$, the groundwater flow within twice the borehole radius will converge through the borehole test section, as illustrated in Figures 4-2 and 4-3.

If there is a disturbed zone around the borehole the correction factor α is given by the radial extent and hydraulic conductivity of the disturbed zone. If the drilling has caused a zone with a lower hydraulic conductivity in the vicinity of the borehole than in the fracture zone, e.g. positive skin due to drilling debris and clogging, the correction factor α will decrease. A zone of higher hydraulic conductivity around the borehole will increase α . Rock stress redistribution, when new boundary conditions are created by the drilling of the borehole, may also change the hydraulic conductivity around the borehole and thus affect α . In Figure 4-3, the correction factor, α , is given as a function of K_2/K_1 at different normalized radial extents of the disturbed zone (r/r_d). If the fracture/fracture zone and groundwater flow are not perpendicular to the borehole axis, this also has to be accounted for. At a 45 degree angle to the borehole axis the value of α will be about 41% larger than in the case of perpendicular flow. This is further discussed in /Gustafsson 2002/ and /Rhén et al. 1991/.

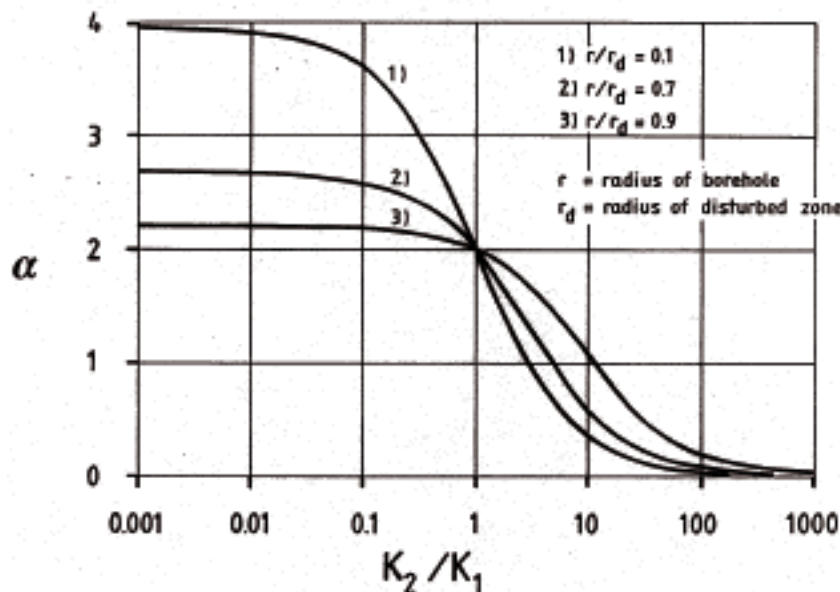


Figure 4-3. The correction factor, α , as a function of K_2/K_1 at different radial extent (r/r_d) of the disturbed zone (skin zone) around the borehole.

In order to obtain the Darcy velocity in the undisturbed rock the calculated ground water flow, Q_w is divided by A, Equation 4-4.

$$v = Q_w/A \quad \text{(Equation 4-4)}$$

The hydraulic gradient is then calculated as

$$I = v/K \quad \text{(Equation 4-5)}$$

where K is the hydraulic conductivity.

4.4.2 The dilution method – evaluation and analysis

The first step of evaluation included studying a graph of the measured concentration versus time data. For further evaluation background concentration, i.e. any tracer concentration in the groundwater before tracer injection, was subtracted from the measured concentrations. Thereafter $\ln(C/C_0)$ was plotted versus time. In most cases that relationship was linear and the proportionality constant was then calculated by performing a linear regression. In the cases where the relationship between $\ln(C/C_0)$ and time was non-linear, a sub-interval was chosen in which the relationship was linear.

The value of $\ln(C/C_0)/t$ obtained from the linear regression was then used to calculate Q_w according to Equation (4-1).

The hydraulic gradient, I, was calculated by combining Equations (4-2), (4-4) and (4-5), and choosing $\alpha = 2$. The hydraulic conductivity, K, in Equation (4-5) was obtained from previously performed POSIVA Difference flow measurements (PFL) /Sokolnicki and Rouhiainen 2005/.

4.4.3 SWIW test – basic outline

A Single Well Injection Withdrawal (SWIW) test may consist of all or some of the following phases:

1. filling-up pressure vessel with groundwater from the selected fracture,
2. injection of water to establish steady state hydraulic conditions (pre-injection),
3. injection of one or more tracers,
4. injection of groundwater (chaser fluid) after tracer injection is stopped,
5. waiting phase,
6. withdrawal (recovery) phase.

The tracer breakthrough data eventually used for evaluation are obtained from the withdrawal phase. The injection of chaser fluid, i.e. groundwater from the pressure vessel, has the effect of pushing the tracer out as a “ring” in the formation surrounding the tested section. This is generally a benefit, because when the tracer is pumped back both ascending and descending parts are obtained in the recovery breakthrough curve. During the waiting phase there is no injection or withdrawal of fluid. The purpose of this phase is to increase the time available for time-dependent transport-processes so that these may be more easily evaluated from the resulting breakthrough curve. A schematic example of a resulting breakthrough curve during a SWIW test is shown in Figure 4-4.

The design of a successful SWIW test requires prior determination of injection and withdrawal flow rates, duration of tracer injection, duration of the various injection, waiting and pumping phases, selection of tracers, tracer injection concentrations, etc.

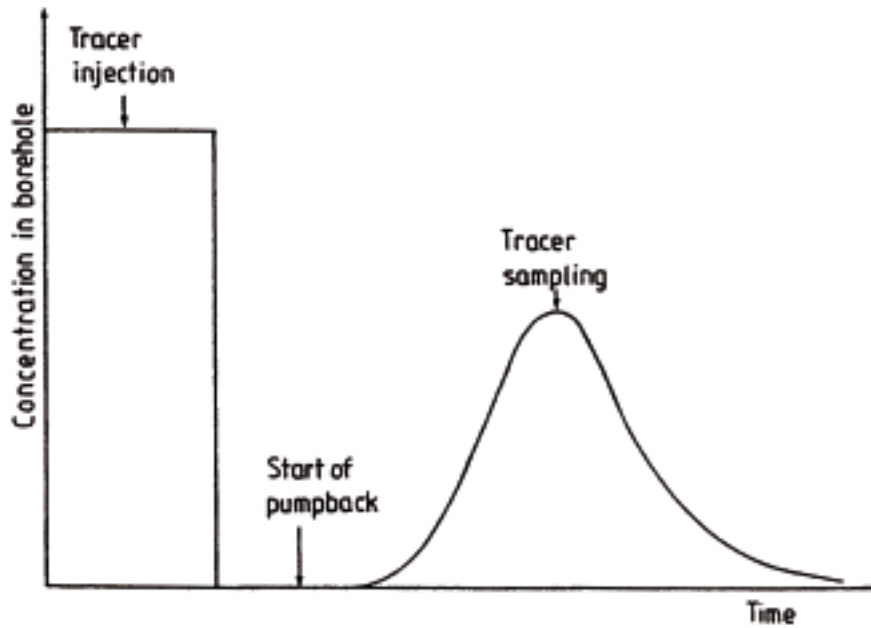


Figure 4-4. Schematic tracer concentration sequence during a SWIW test /Andersson 1995/.

4.4.4 SWIW test – evaluation and analysis

The model evaluation of the experimental results was carried out assuming homogenous conditions. Model simulations were made using the model code SUTRA /Voss 1984/ and the experiments were simulated without a background hydraulic gradient. It was assumed that flow and transport occur within a planar fracture zone of some thickness. The volume available for flow was represented by assigning a porosity value to the assumed zone. Modelled transport processes include advection, dispersion and linear equilibrium sorption.

The sequence of the different injection phases were modelled as accurately as possible based on supporting data for flows and tracer injection concentration. Generally, experimental flows and times may vary from one phase to another, and the flow may also vary within phases. The specific experimental sequences for the borehole sections are listed in Table 5-2.

In the simulation model, tracer injection was simulated as a function accounting for mixing in the borehole section and sorption (for cesium and rubidium) on the borehole walls. The function assumes a completely mixed borehole section and linear equilibrium surface sorption:

$$C = (C_0 - C_{in})e^{-\left(\frac{Q}{V_{bh} + K_a A_{bh}}\right)t} + C_{in} \quad \text{(Equation 4-6)}$$

where C is concentration in water leaving the borehole section, and entering the formation (kg/m^3), V_{bh} is the borehole volume including circulation tubes (m^3), A_{bh} is area of borehole walls (m^2), Q_{in} is flow rate (m^3/s), C_{in} is concentration in the water entering the borehole section (kg/m^3), C_0 is initial concentration in the borehole section (kg/m^3), K_a is surface sorption coefficient (m) and t is elapsed time (s).

Based on in-situ experiments /Andersson et al. 2002/ and laboratory measurements on samples of crystalline rock /Byegård and Tullborg 2005/ the sorption coefficient K_a was assigned a value of 10^{-2} m in all simulations. An example of the tracer injection input function is given in Figure 4-5, showing a 50 minutes long tracer injection phase followed by a chaser phase.

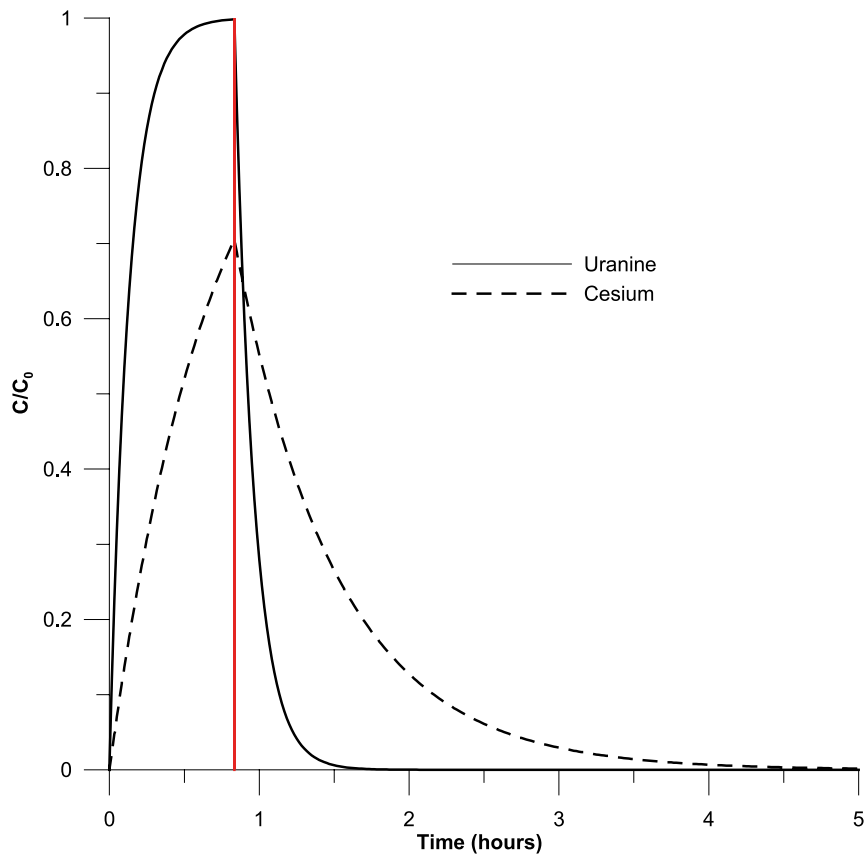


Figure 4-5. Example of simulated tracer injection functions for a tracer injection phase (ending at 50 minutes shown by the vertical red line) immediately followed by a chaser phase.

Non-linear regression was used to fit the simulation model to experimental data. The estimation strategy was generally to estimate the dispersivity (a_L) and a retardation factor (R), while setting the porosity (i.e. the available volume for flow) to a fixed value. Simultaneous fitting of both tracer breakthrough curves (Uranine and cesium in the example), and calculation of fitting statistics, was carried out using the approach described in /Nordqvist and Gustafsson 2004/. Tracer breakthrough curves for Uranine and rubidium are related and calculated in the same way.

4.5 Nonconformities

The inclination of the borehole varies from 60 degrees from the horizontal plane at the surface to 36 degrees at 1,000 m borehole length. The pressure gauge shows how deep from the ground surface the transmitter, i.e. the dilution probe, is located. In this case the inclination of the borehole entails that the deviation between borehole length and the depth from the ground surface increase further down the borehole.

KFM08A is located near the sea and is quite sensitive to variations in air pressure and sea level. This is shown in the dilution measurement in section 685.5–688.5 m where the pressure is increasing due to an increase in air pressure. The pressure increase might give an increase of the dilution and consequently an apparent larger groundwater flow.

The reference marks at 151, 450, 500 and 552 m could not be detected. Reference marks at 200 and 250 m were used for dilution measurement at 188.5–191.5 m and reference marks at 250 and 600 m were used for the dilution measurement at 479.0–482.0 m.

After pumping water from the test section to the SWIW tank, the pressure in the section was lowered 300 kPa and the recovery of pressure took 10 days. To reduce the pressure recovery time the packers were deflated. Borehole water was then entering the section before the SWIW test. The increase in conductivity indicates that the borehole water originates from the part of borehole below the section. This water presumably has a higher background of cesium and rubidium than the fractures in the test section.

A number of the samples taken for Uranin analysis for the SWIW test are discoloured due to sedimentation and cannot be used for evaluation.

The borehole dimension was measured with an acoustic caliper method. It has recently been found that this method not is as accurate as required due to lack of exactness in calibration of the caliper devices. Since the groundwater flow is determined from the dilution curve and the calculated water volume in the test section, according to Equation 4-1, impeccable measure of the borehole diameter is of great importance. Because of the uncertainty in the caliper method, the nominal borehole diameter is used for the final calculations of groundwater flow, Darcy velocity and hydraulic gradient presented in this report.

No deviations were made from to the activity plan or the method description. The nonconformities described above are caused by external conditions.

5 Results

The primary data and original results are stored in the SKB database SICADA, where they are traceable by Activity Plan number. These data shall be used for further interpretation or modelling.

5.1 Dilution measurements

Figure 5-1 exemplifies a typical dilution curve in a fracture zone straddled by the test section at 274.5–277.5 m borehole length in borehole KFM08A. In the first phase the background value is recorded for about 30 minutes. In phase two Uranine tracer is injected and after mixing, a start concentration (C_0) of about 1.20 mg/l is achieved. In phase three the dilution is measured for about 43 hours. Thereafter the packers are deflated and the remaining tracer flows out of the test section. Figure 5-2 shows the measured pressure during the dilution measurement. Since the pressure gauge is positioned about seven metres from top of test section there is a bias from the pressure in the test section which is not corrected for, as only changes and trends relative to the start value are of great importance for the dilution measurement. Figure 5-3 is a plot of the $\ln(C/C_0)$ versus time data and linear regression best fit to data showing a good fit with correlation $R^2 = 0.9950$. The standard deviation, STDAV, shows the mean divergence of the values from the best fit line and is calculated from

$$\text{STDAV} = \sqrt{\frac{n \sum x^2 - (\sum x)^2}{n(n-1)}}$$

Calculated groundwater flow rate, Darcy velocity and hydraulic gradient are presented in Table 5-1 together with the results from all other dilution measurements carried out in borehole KFM08A.

The dilution measurements were carried out with the dye tracer Uranine. Uranine normally has a low and constant background concentration and the tracer can be injected and measured in concentrations far above the background value, which gives a large dynamic range and accurate flow determinations.

Details of all dilution measurements and evaluations, with diagrams of dilution versus time and the supporting parameters pressure, temperature and circulation flow rate are presented in Appendix B1–B5.

KFM08A 274.5-277.5 m

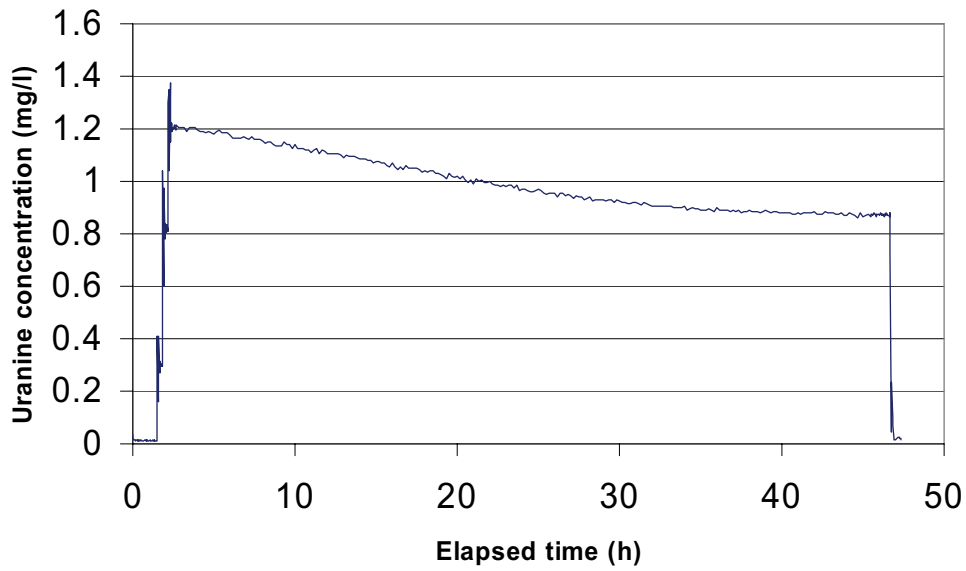


Figure 5-1. Dilution measurement in borehole KFM08A, section 274.5–277.5 m.

KFM08A 274.5-277.5 m

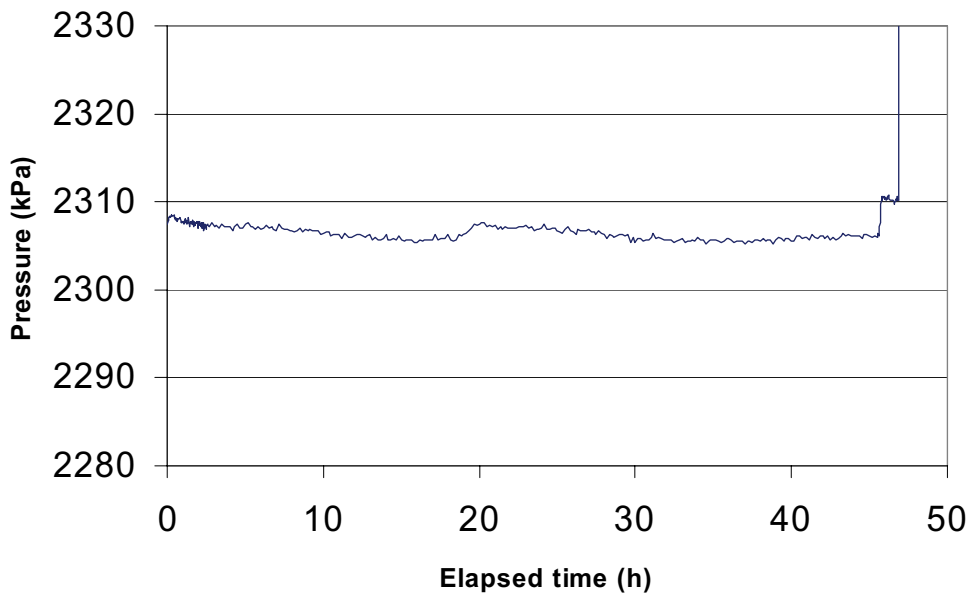


Figure 5-2. Measured pressure during dilution measurement in borehole KFM08A, section 274.5–277.5 m.

KFM08A 274.5-277.5 m

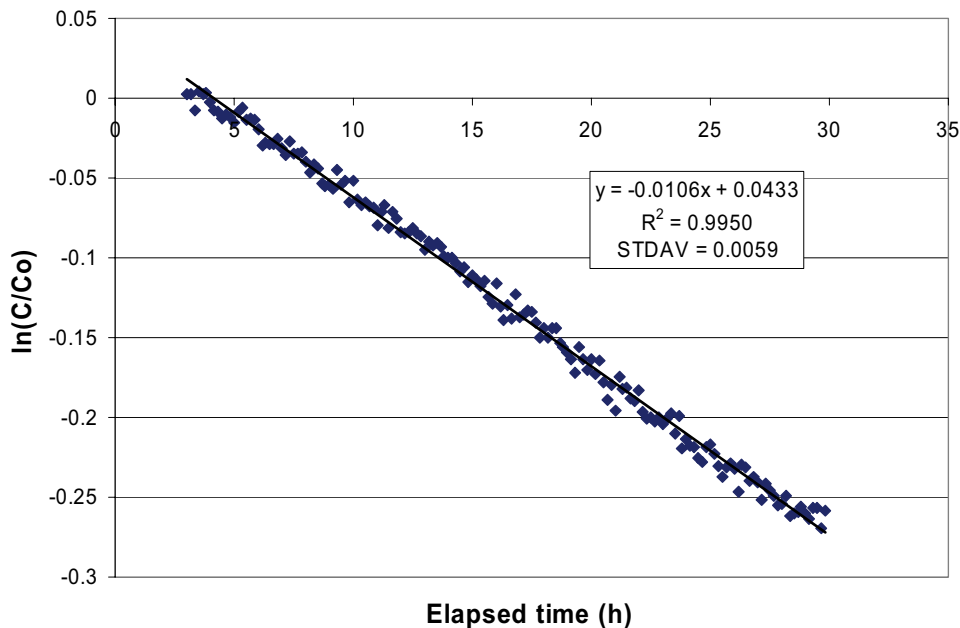


Figure 5-3. Linear regression best fit to data from dilution measurement in borehole KFM08A, section 274.5–277.5 m.

5.1.1 KFM08A, section 188.5–191.5 m

This dilution measurement was carried out in a single flowing fracture with the dye tracer Uranine. The complete test procedure can be followed in Figure 5-4. Background concentration (0.03 mg/l) is measured for about 30 minutes. Thereafter the Uranine tracer is injected and after mixing it finally reaches a start concentration of 1.08 mg/l above background. Dilution is measured for about 65 hours, the packers are then deflated. Hydraulic pressure is stable but shows small diurnal pressure variations due to earth tidal effects (Appendix B1). The concentration reaches a level near background at the end of the dilution measurement. For this reason the latter part was excluded and the final evaluation was made on the 5 to 40 hours part of the dilution curve. The regression line fits well to the slope of the dilution with a correlation coefficient of $R^2 = 0.9976$ for the best fit line (Figure 5-5). The groundwater flow rate, calculated from the best fit line, is 2.21 ml/min. Calculated hydraulic gradient is 0.11 and Darcy velocity $8.0 \cdot 10^{-8}$ m/s. The hydraulic gradient is large and may be caused by local effects, where the measured fracture constitutes a hydraulic conductor between other fractures with different hydraulic heads, or wrong estimates of the correction factor, α , and/or the hydraulic conductivity of the fracture.

KFM08A 188.5-191.5 m

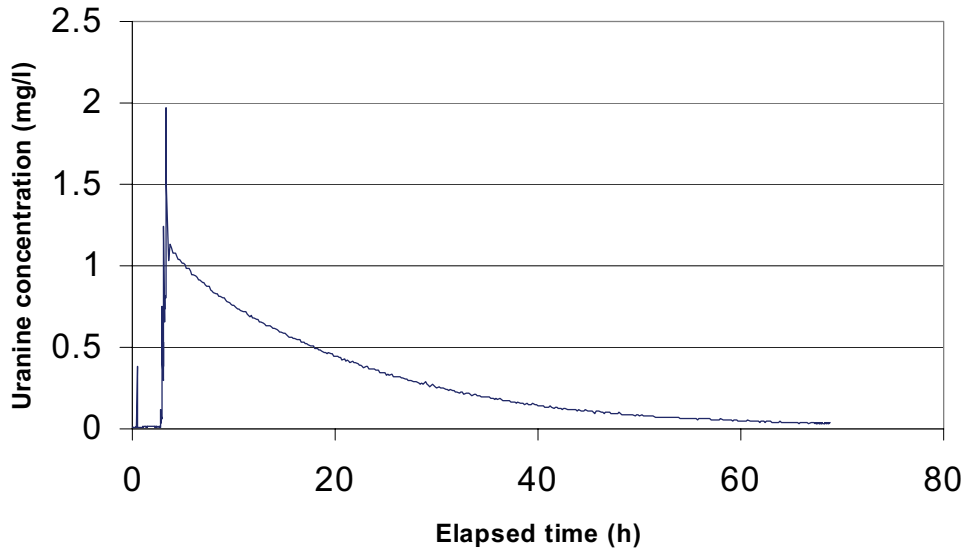


Figure 5-4. Dilution measurement in borehole KFM08A, section 188.5–191.5 m.

KFM08A 188.5-191.5 m

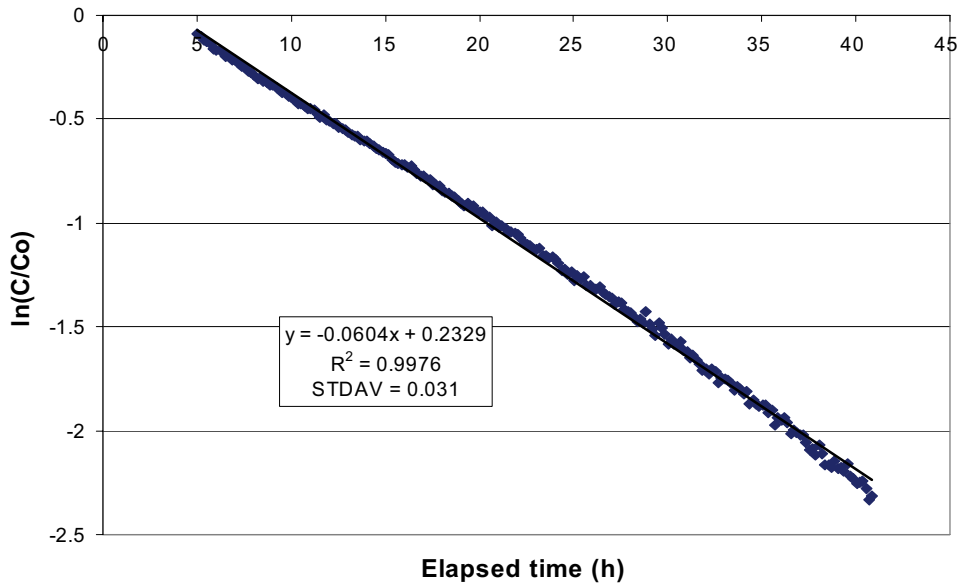


Figure 5-5. Linear regression best fit to data from dilution measurement in borehole KFM08A, section 188.5–191.5 m.

5.1.2 KFM08A, section 274.5–277.5 m

This dilution measurement was carried out with the dye tracer Uranine in a test section with three – four flowing fractures. The background measurement, tracer injection and dilution can be followed in Figure 5-6. Background concentration is 0.01 mg/l. The Uranine tracer is injected and after mixing it reaches a start concentration of 1.19 mg/l above background. Dilution is measured for about 43 hours, thereafter the packers are deflated and the remaining tracer flows out of the test section. A diurnal pressure variation due to earth tidal effects is visible and pressure shows a slight decreasing trend the first 10 hours (Appendix B2). The complete set of the $\ln(C/C_0)$ versus time data could not fit a straight line, although the correlation coefficient was high ($R^2 = 0.9663$). For this reason the final evaluation was made on the first part of the dilution measurement, from 3 to 30 hours of elapsed time. The correlation coefficient of the best fit line is $R^2 = 0.9950$ (Figure 5-7), and the groundwater flow rate, calculated from the best fit line, is 0.39 ml/min. Calculated hydraulic gradient is 0.033 and Darcy velocity $1.40 \cdot 10^{-8}$ m/s.

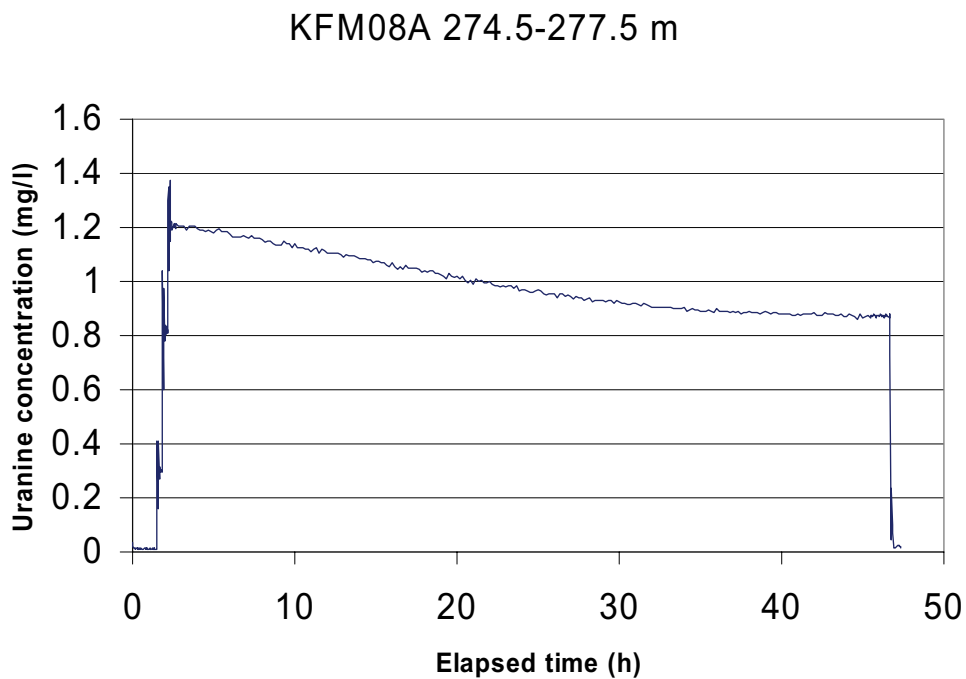


Figure 5-6. Dilution measurement in borehole KFM08A, section 274.5–277.5 m.

KFM08A 274.5-277.5 m

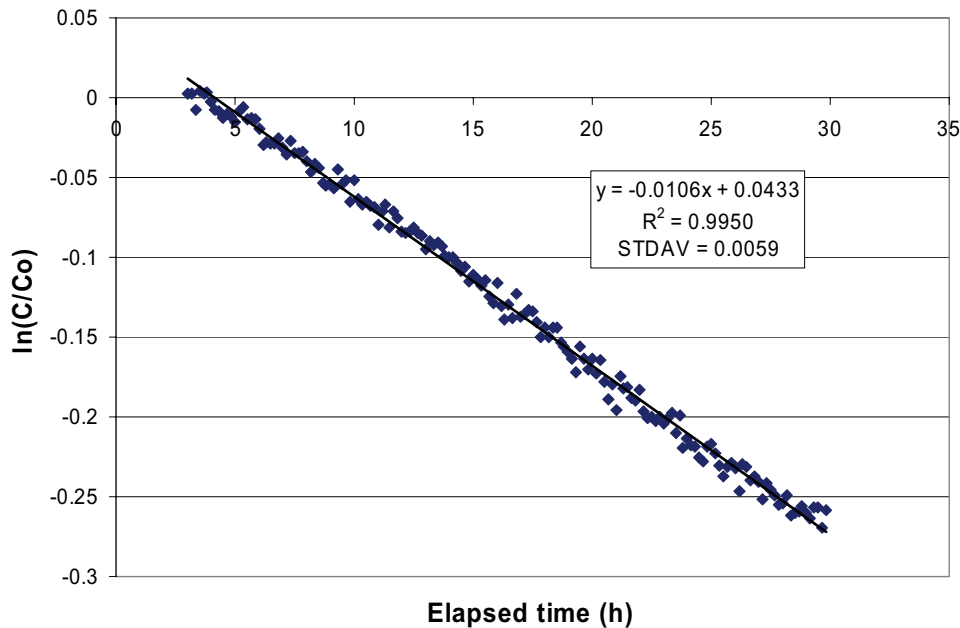


Figure 5-7. Linear regression best fit to data from dilution measurement in borehole KFM08A, section 274.5–277.5 m.

5.1.3 KFM08A, section 410.5–413.5 m

This dilution measurement was carried out with the dye tracer Uranine in a test section with three flowing fractures. The background measurement, tracer injection and dilution can be followed in Figure 5-8. Background concentration is 0.01 mg/l. The Uranine tracer is injected in two steps and after mixing it reaches a start concentration of 0.93 mg/l above background. Dilution is measured for about 138 hours. Thereafter the packers are deflated and the remaining tracer flows out of the test section. Hydraulic pressure shows a decreasing trend and small diurnal pressure variations due to earth tidal effects (Appendix B3). The final evaluation was made from 75 to 140 hours of elapsed time when the pressure is nearly stabilised. The regression line fits well to the slope of the dilution with a correlation coefficient of $R^2 = 0.9878$ for the best fit line (Figure 5-9). The groundwater flow rate, calculated from the best fit line, is 0.10 ml/min. Calculated hydraulic gradient is 0.95 and Darcy velocity $1.6 \cdot 10^{-9}$ m/s. The hydraulic gradient is very large and may be caused by local effects where the measured fractures constitute hydraulic conductors between other fractures with different hydraulic heads or wrong estimates of the correction factor, α , and/or the hydraulic conductivity of the fracture. The pressure decrease at the beginning of the measurement may give some contribution to groundwater flow rate and hence to the large calculated hydraulic gradient. The hydraulic transmissivity of the section is also at the lower limit of the measurement range for the dilution probe which may decrease accuracy in determined groundwater flow rate.

KFM08A 410.5 - 413.5 m

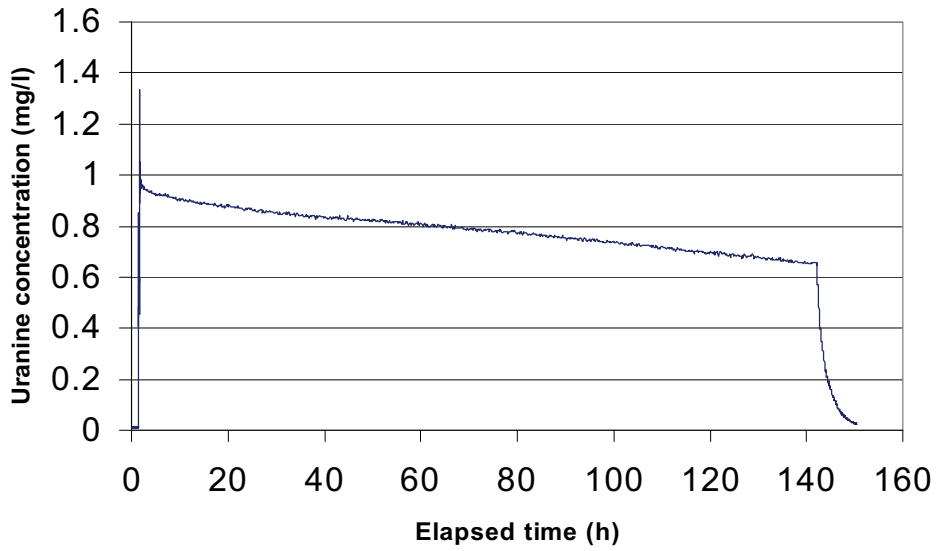


Figure 5-8. Dilution measurement in borehole KFM08A, section 410.5–413.5 m.

KFM08A 410.5 - 413.5 m

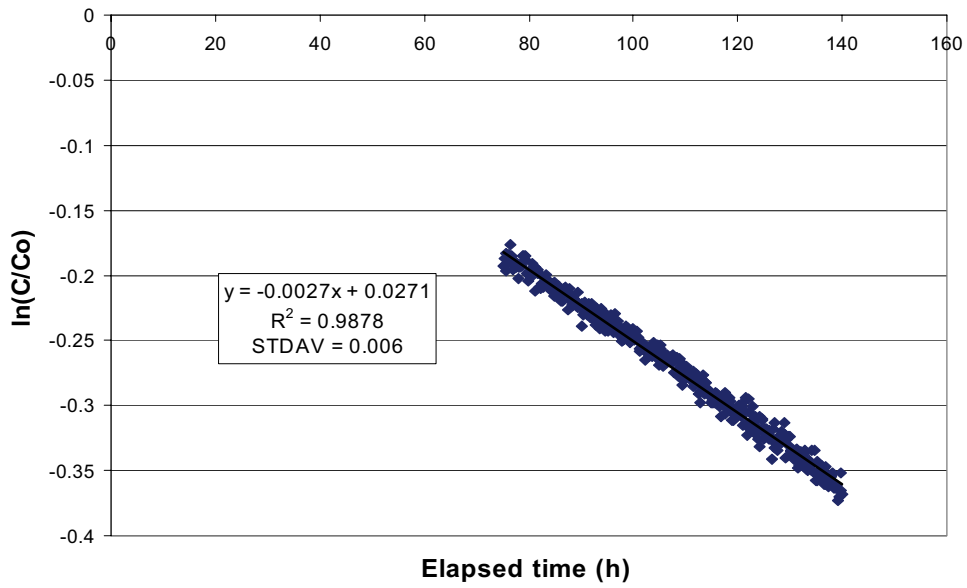


Figure 5-9. Linear regression best fit to data from dilution measurement in borehole KFM08A, section 410.5–413.5 m.

5.1.4 KFM08A, section 479.0–482.0 m

This dilution measurement was carried out with the dye tracer Uranine in a test section with one-two flowing fractures. The background measurement, tracer injection and dilution can be followed in Figure 5-10. Background concentration (0.02 mg/l) is measured for about 30 minutes. Thereafter the Uranine tracer is injected in three steps and after mixing it finally reaches a start concentration of 0.95 mg/l above background. Dilution is measured for about 69 hours. Thereafter the packers are deflated and the remaining tracer flows out of the test section. Hydraulic pressure shows a slow decreasing trend and small diurnal pressure variations due to earth tidal effects (Appendix B4). Because of the decreasing trend in hydraulic pressure, the final evaluation was made on the last part of the dilution measurement, from 35 to 75 hours of elapsed time where the pressure is at the most stable part of the dilution measurement. The regression line shows an acceptable fit to the $\ln(C/C_0)$ versus time data with a correlation coefficient of $R^2 = 0.7530$ for the best fit line (Figure 5-11). The groundwater flow rate, calculated from the best fit line, is 0.026 ml/min. Calculated hydraulic gradient is 0.040 and Darcy velocity $9.3 \cdot 10^{-10}$ m/s.

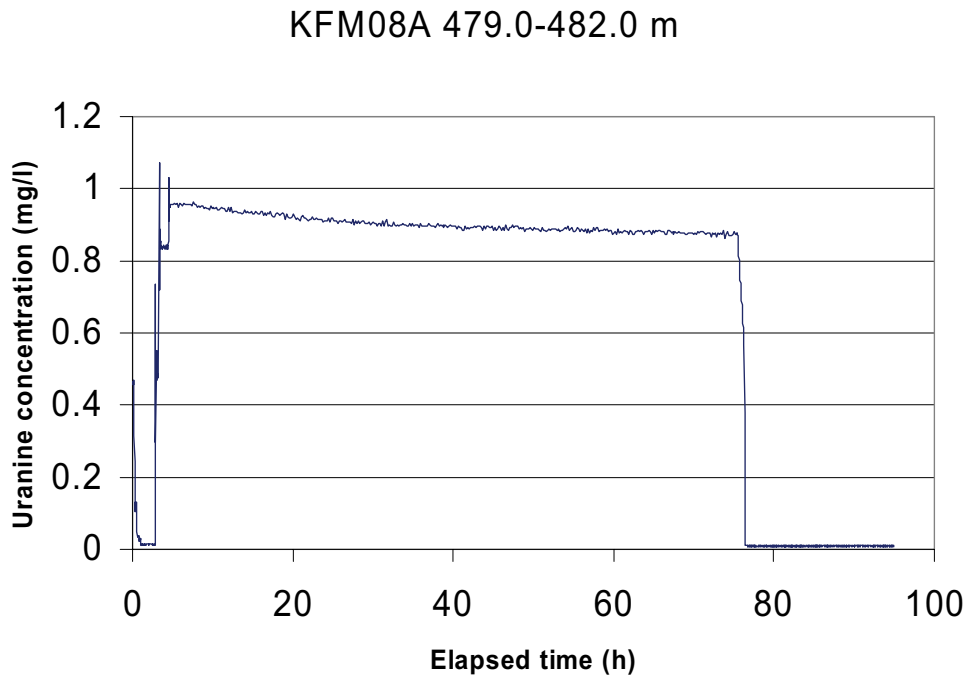


Figure 5-10. Dilution measurement in borehole KFM08A, section 479.0–482.0 m.

KFM08A 479.0-482.0 m

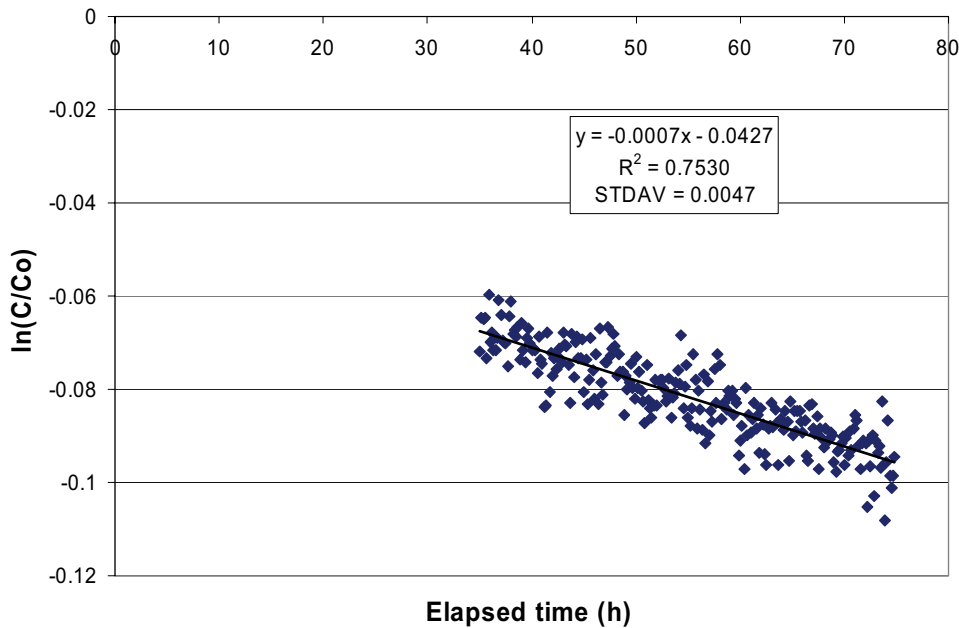


Figure 5-11. Linear regression best fit to data from dilution measurement in borehole KFM08A, section 479.0–482.0 m.

5.1.5 KFM08A, section 685.5–688.5 m

This dilution measurement was carried out with the dye tracer Uranine in a test section with a single flowing fracture. The background measurement, tracer injection and dilution can be followed in Figure 5-12. Background concentration is 0.01 mg/l. The Uranine tracer is injected and after mixing it reaches a start concentration of 0.97 mg/l above background. Dilution is measured for about 114 hours. Thereafter the packers are deflated. Hydraulic pressure shows an increasing trend due to an increase in air pressure (Appendix B5). The final evaluation was made on the last part of the dilution measurement, from 90 to 117 hours of elapsed time, where the hydraulic pressure is at the most stable part of the dilution measurement. The regression line fits well to the slope of the dilution with a correlation coefficient of $R^2 = 0.9819$ for the best fit line (Figure 5-13). The groundwater flow rate, calculated from the best fit line, is 0.25 ml/min. Calculated hydraulic gradient is 0.019 and Darcy velocity $9.1 \cdot 10^{-9}$ m/s.

KFM08A 685.5 - 688.5 m

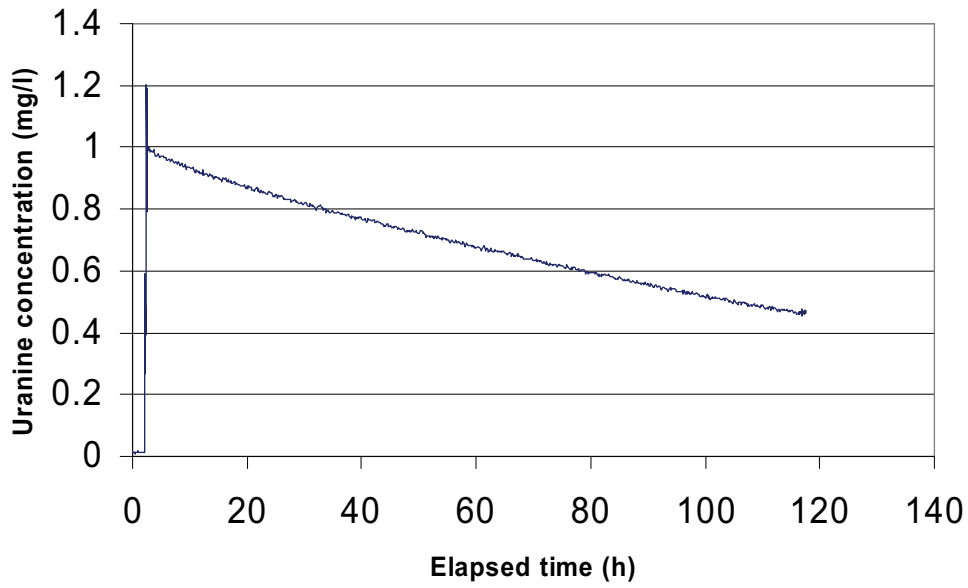


Figure 5-12. Dilution measurement in borehole KFM08A, section 685.5–688.5 m.

KFM08A 685.5 - 688.5 m

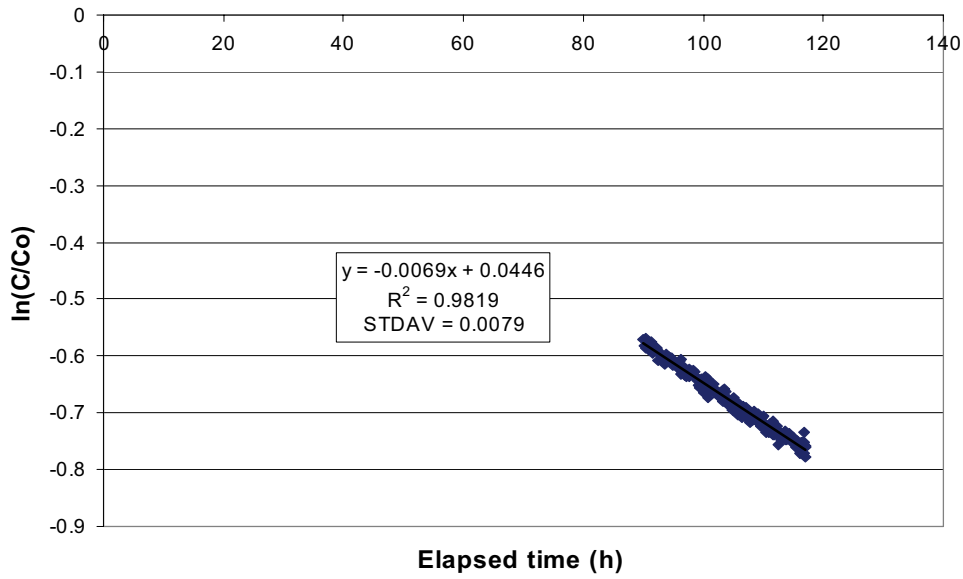


Figure 5-13. Linear regression best fit to data from dilution measurement in borehole KFM08A, section 685.5–688.5 m.

5.1.6 Summary of dilution results

Calculated groundwater flow rate, Darcy velocity and hydraulic gradient from all dilution measurements carried out in borehole KFM08A are presented in Table 5-1.

The results show that the groundwater flow varies considerably in fractures and fracture zones during natural, i.e. undisturbed, conditions, with flow rates from 0.03 to 2.21 ml/min and Darcy velocities from $9.3 \cdot 10^{-10}$ to $8.0 \cdot 10^{-8}$ m/s. The highest flow rates are measured in the shallow sections and the flow rates decrease with depth, Figure 5-14. Exception is the section at c. 685 m borehole length where the flow is high in spite of the depth and the single fracture. However, hydraulic transmissivity is high. The Darcy velocity follows the same trend as the flow rates, Figure 5-15. A large portion of the measured fractures/fracture zones are within a small range of transmissivity, however correlation between flow rate and transmissivity is indicated in Figure 5-17, with the highest flow rates at high transmissivity. Hydraulic gradients, calculated according to the Darcy concept, are large in the single fracture section at c. 188 m and in the minor fracture zone at c. 410 m borehole length, Figure 5-16. In the other measured fractures/fracture zones the hydraulic gradient is within the expected range. It is not clear if the large gradients are caused by local effects where the measured fracture constitutes a hydraulic conductor between other fractures with different hydraulic heads or due to wrong estimates of the correction factor, α , and/or the hydraulic conductivity of the fracture. The pressure decrease at the beginning of the measurement at c. 410 m may give some contribution to the measured groundwater flow rate and hence to the large calculated hydraulic gradient. The hydraulic transmissivity of the section is also at the lower limit of the measurement range for the dilution probe which may decrease accuracy in determined groundwater flow rate.

Table 5-1. Groundwater flow, Darcy velocities and Hydraulic gradients for all measured sections in borehole KFM08A.

Borehole	Test section (m)	Number of flowing fractures*	T (m ² /s)*	Q (ml/min)	Q (m ³ /s)	Darcy velocity (m/s)	Hydraulic gradient
KFM08A	188.5–191.5	1	2.20E–06	2.21	3.7E–08	8.0E–08	0.11
KFM08A	274.5–277.5	3–4	1.29E–06	0.39	6.5E–09	1.4E–08	0.033
KFM08A	410.5–413.5	3	1.13E–08	0.10	1.6E–09	3.6E–09	0.95
KFM08A	479.0–482.0	1–2	6.93E–08	0.026	4.3E–10	9.3E–10	0.040
KFM08A	685.5–688.5	1	1.41E–06	0.25	4.2E–09	9.1E–09	0.019

* /Sokolnicki and Rouhiainen 2005/.

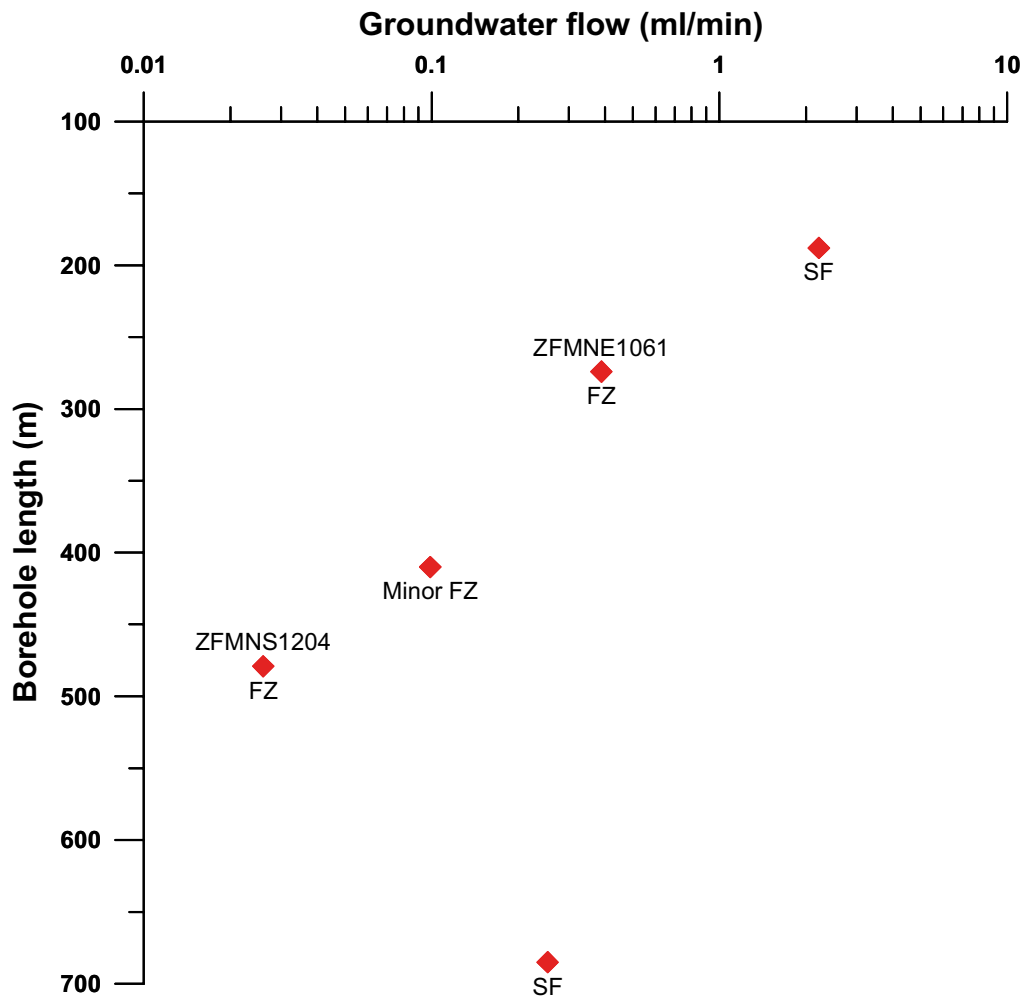


Figure 5-14. Groundwater flow versus borehole length during undisturbed, i.e. natural hydraulic gradient conditions. Results from dilution measurements in single fractures (SF) and fracture zones (FZ) in borehole KFM08A. Numbered labels refer to fracture zone notation in the Forsmark site description model SDM F2.1 /SKB 2006/.

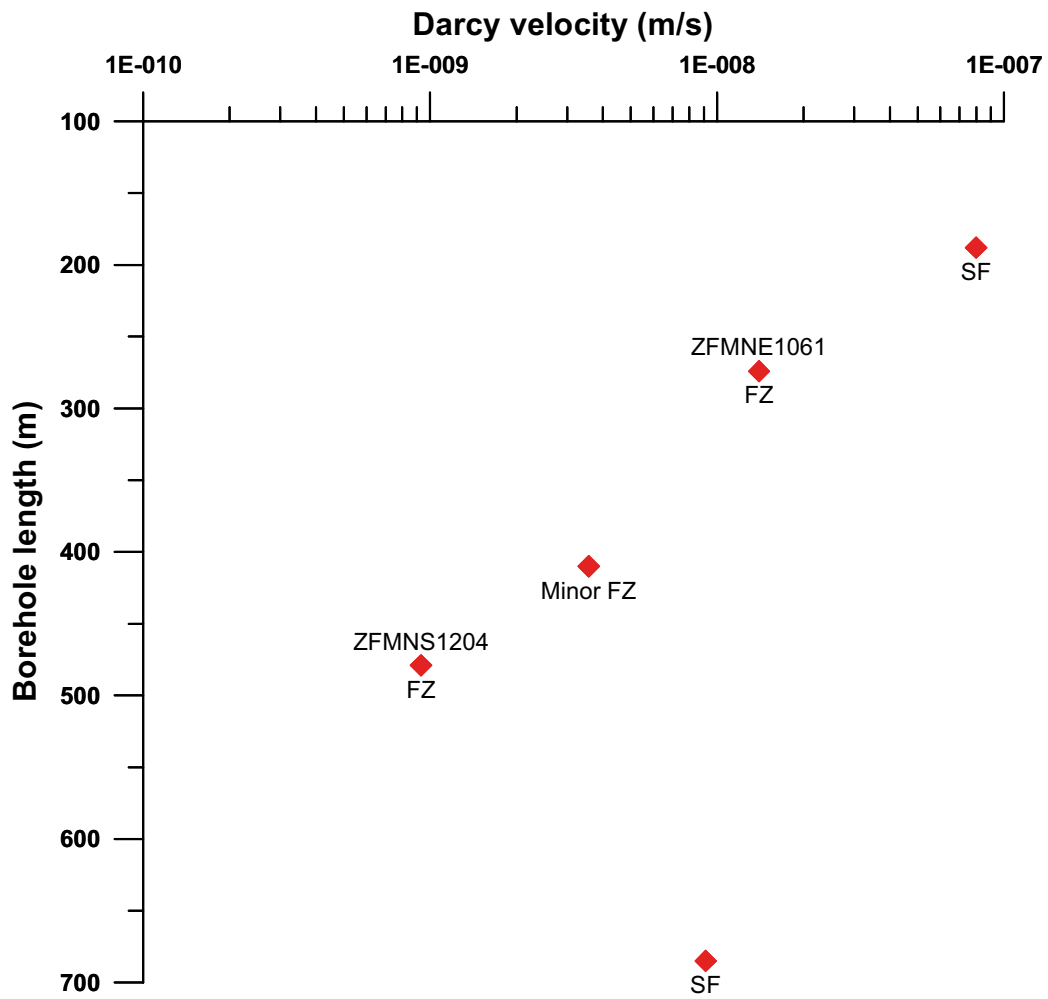


Figure 5-15. Darcy velocity versus borehole length during undisturbed, i.e. natural hydraulic gradient conditions. Results from dilution measurements in single fractures (SF) and fracture zones (FZ) in borehole KFM08A. Numbered labels refer to fracture zone notation in the Forsmark site description model SDM F2.1 /SKB 2006/.

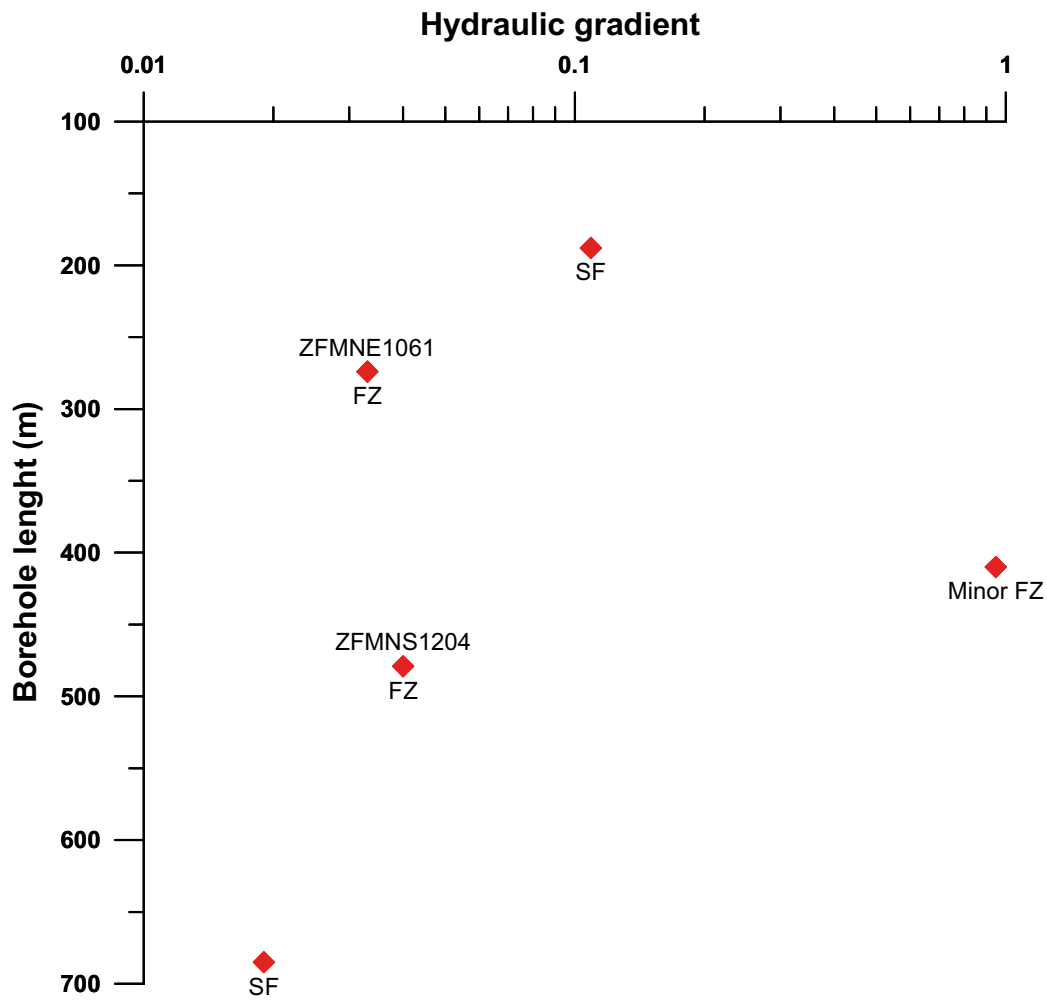


Figure 5-16. Hydraulic gradient versus versus borehole length during undisturbed, i.e. natural hydraulic gradient conditions. Results from dilution measurements in single fractures (SF) and fracture zones (FZ) in borehole KFM08A. Numbered labels refer to fracture zone notation in the Forsmark site description model SDM F2.1 /SKB 2006/.

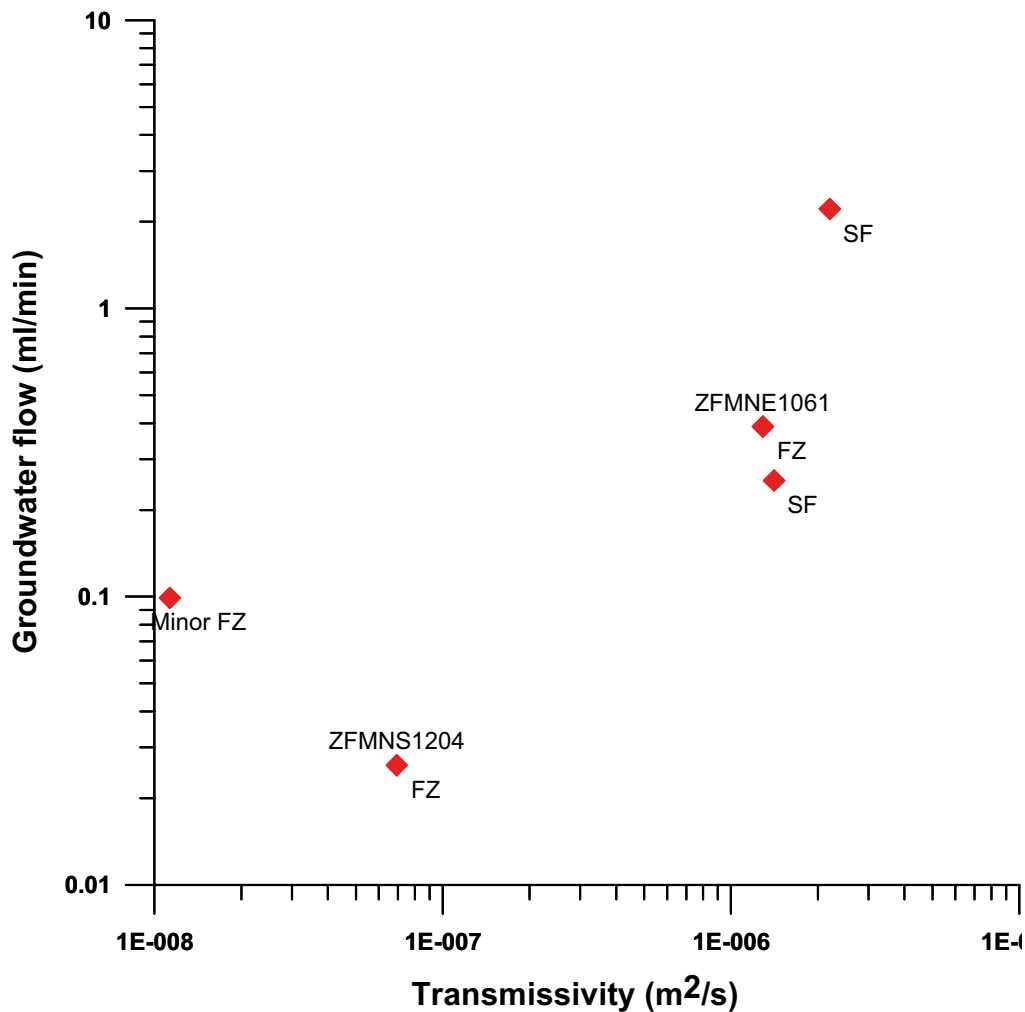


Figure 5-17. Groundwater flow versus transmissivity during undisturbed, i.e. natural hydraulic gradient conditions. Results from dilution measurements in single fractures (SF) and fracture zones (FZ) in borehole KFM08A. Numbered labels refer to fracture zone notation in the Forsmark site description model SDM F2.1 /SKB 2006/.

5.2 SWIW test

5.2.1 Treatment of experimental data

The experimental data presented in this section have been corrected for background concentrations. Sampling times have been adjusted to account for residence times in injection and sampling tubing. Thus, time zero in all plots refers to when the fluid containing the tracer mixture starts to enter the tested borehole section.

5.2.2 Tracer recovery breakthrough in KFM08A, 410.5–413.5 m

Durations and flows for the various experimental phases are summarised in Table 5-2.

The experimental breakthrough curves from the recovery phase for Uranine, cesium and rubidium, respectively, are shown in Figures 5-18a, 5-18b and 5-18c. The time coordinates are corrected for residence time in the tubing, as described above, and concentrations are normalised through division by the total injected tracer mass.

Table 5-2. Durations (hours) and fluid flows (l/h) during various experimental phases for section 410.5–413.5 m. All times have been corrected for tubing residence time such that time zero refers to the time when the tracer mixture starts to enter the tested borehole section.

Phase	Start (h)	Stop (h)	Volume (l)	Average flow (l/h)	Cumulative injected volume (l)
Pre-injection	-5.04	0.00	12.88	2.55	12.9
Tracer injection	0.00	4.52	11.03	2.44	23.9
Chaser injection	4.52	70.57	161.2	2.44	185.1
Recovery	70.57	425.06	977.6	2.30	

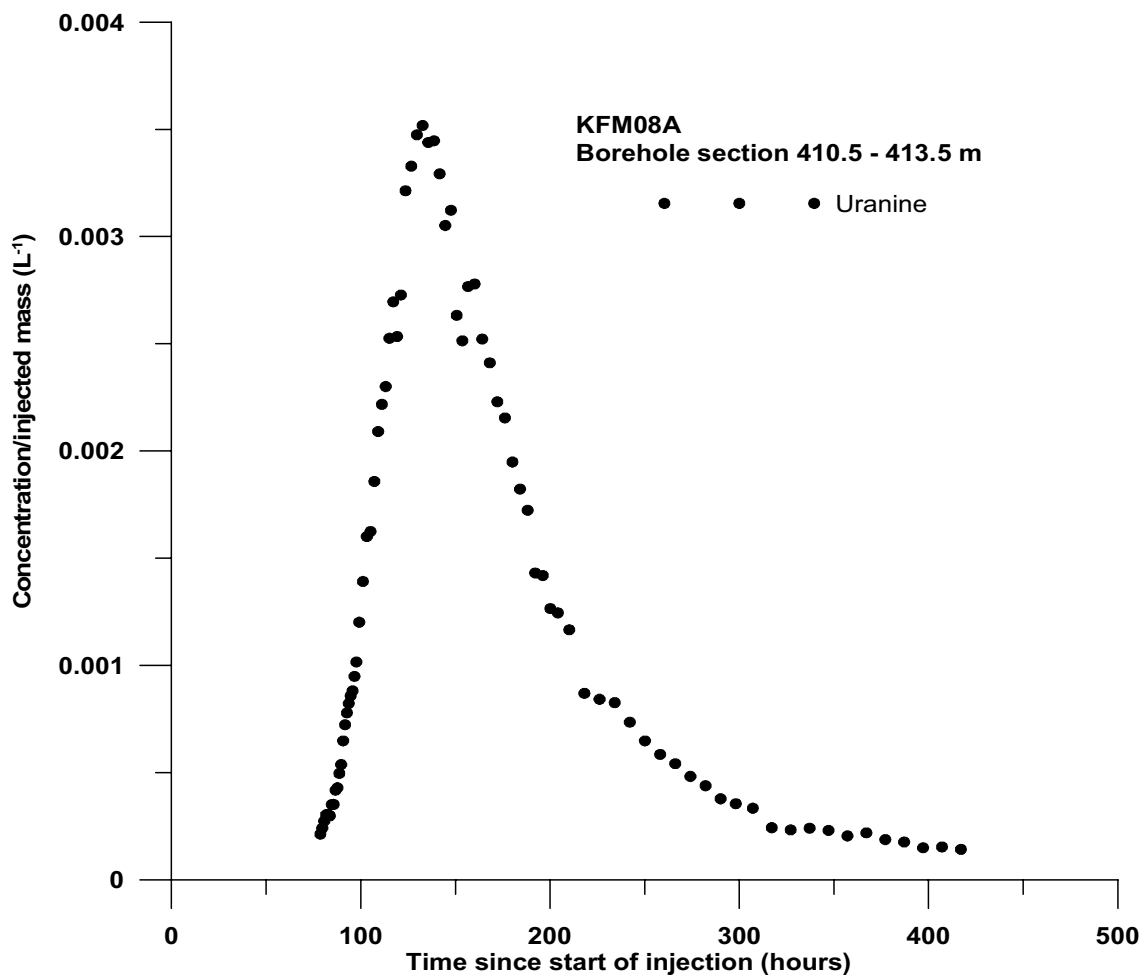


Figure 5-18a. Normalised recovery phase breakthrough curve for Uranine in section 410.5–413.5 m in borehole KFM08A.

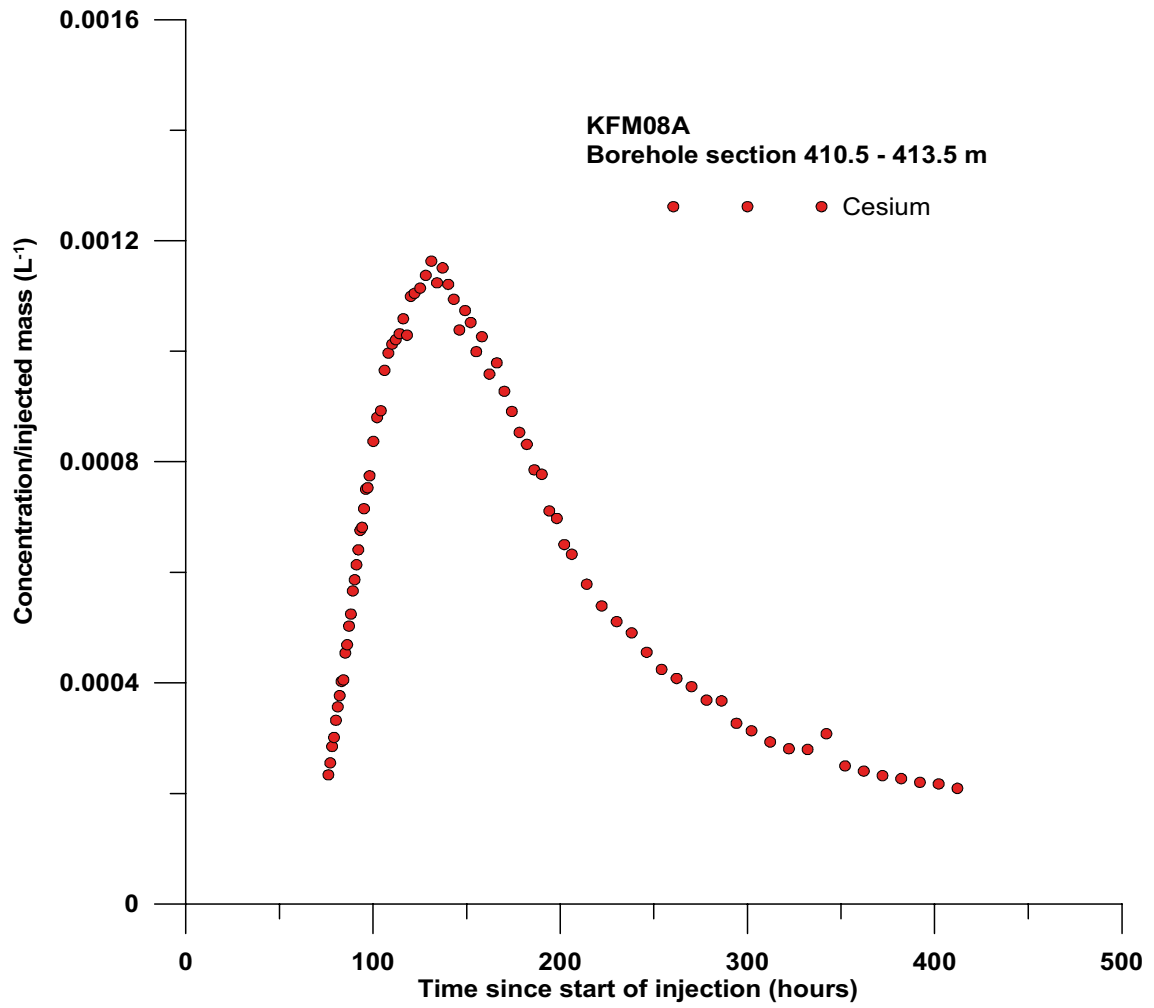


Figure 5-18b. Normalised recovery phase breakthrough curve for cesium in section 410.5–413.5 m in borehole KFM08A.

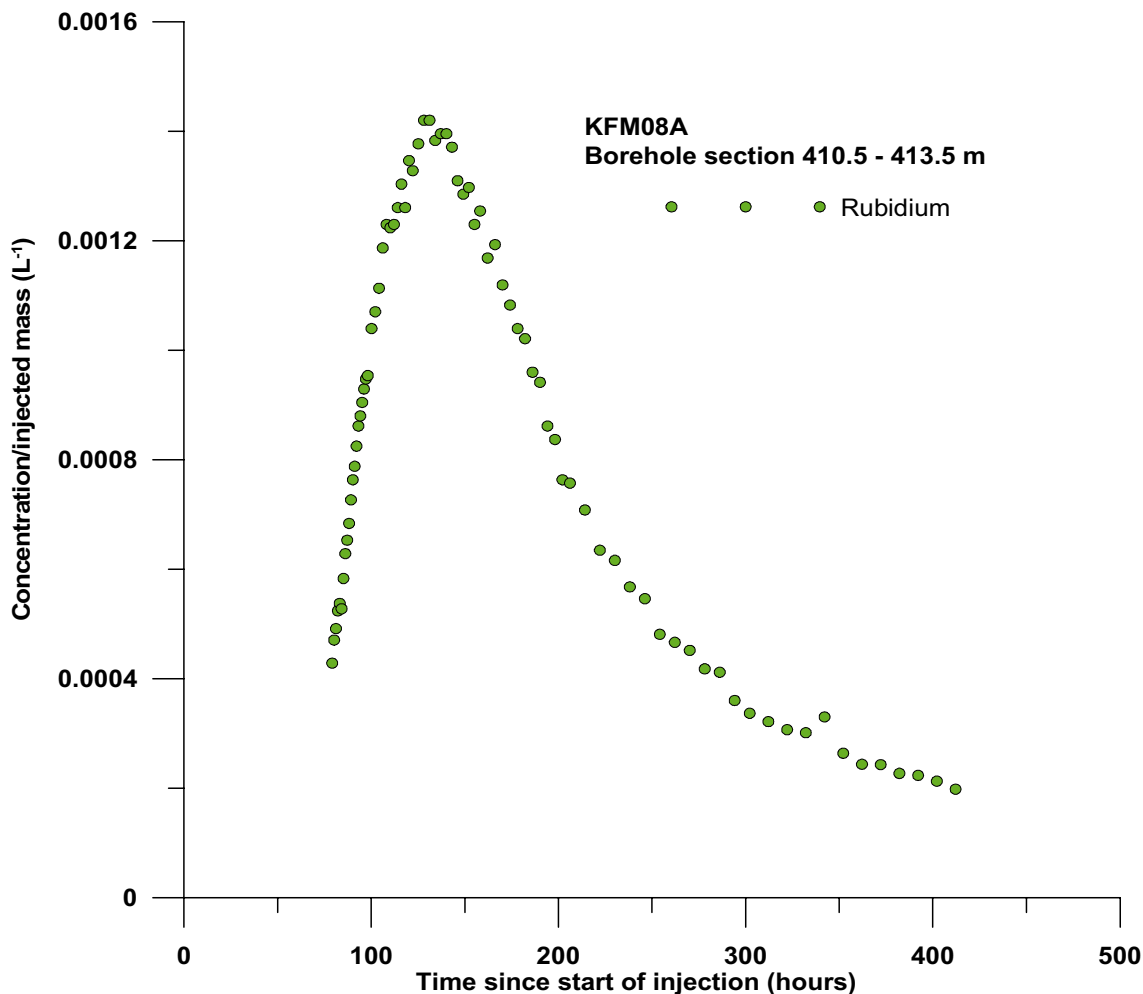


Figure 5-18c. Normalised recovery phase breakthrough curve for rubidium in section 410.5–413.5 m in borehole KFM08A.

Normalised breakthrough curves (concentration divided by total injected tracer mass) for the three different tracers are plotted together in Figure 5-19. The figure shows that the tracers behave in different ways, presumably caused by different sorption properties. Approximately, the breakthrough curves appear to conform to what would be expected from a SWIW test using tracers of different sorption properties. The considerable difference between Uranine and the two other curves may also be seen as an indication of a relatively strong sorption effect for rubidium and cesium. The figure indicates similar tracer behaviour as in KLX03 /Gustafsson et al. 2006/ as well as in KFM02A and KFM03A /Gustafsson et al. 2005/.

The tracer recovery from the recovery phase pumping is rather difficult to estimate from the experimental breakthrough curves, because the tailing parts appear to continue well beyond the last sampling time. Preliminary estimation of recovery from the experimental breakthrough curves at the last sampling time yields values of 81.1%, 50.1% and 42.4% for Uranine, cesium and rubidium, respectively. These estimates are based on the average flow rate during the recovery phase.

Final tracer recovery values, i.e. that would have resulted if pumping had been allowed to continue until tracer concentrations had decreased to background values, are difficult to estimate from the experimental curves. However, plausible visual extrapolations of the curves do not clearly indicate incomplete recovery and that the tracer recovery would differ among the three tracers. Thus, for the subsequent model evaluation, it is assumed that tracer recovery is the same for all of the tracers.

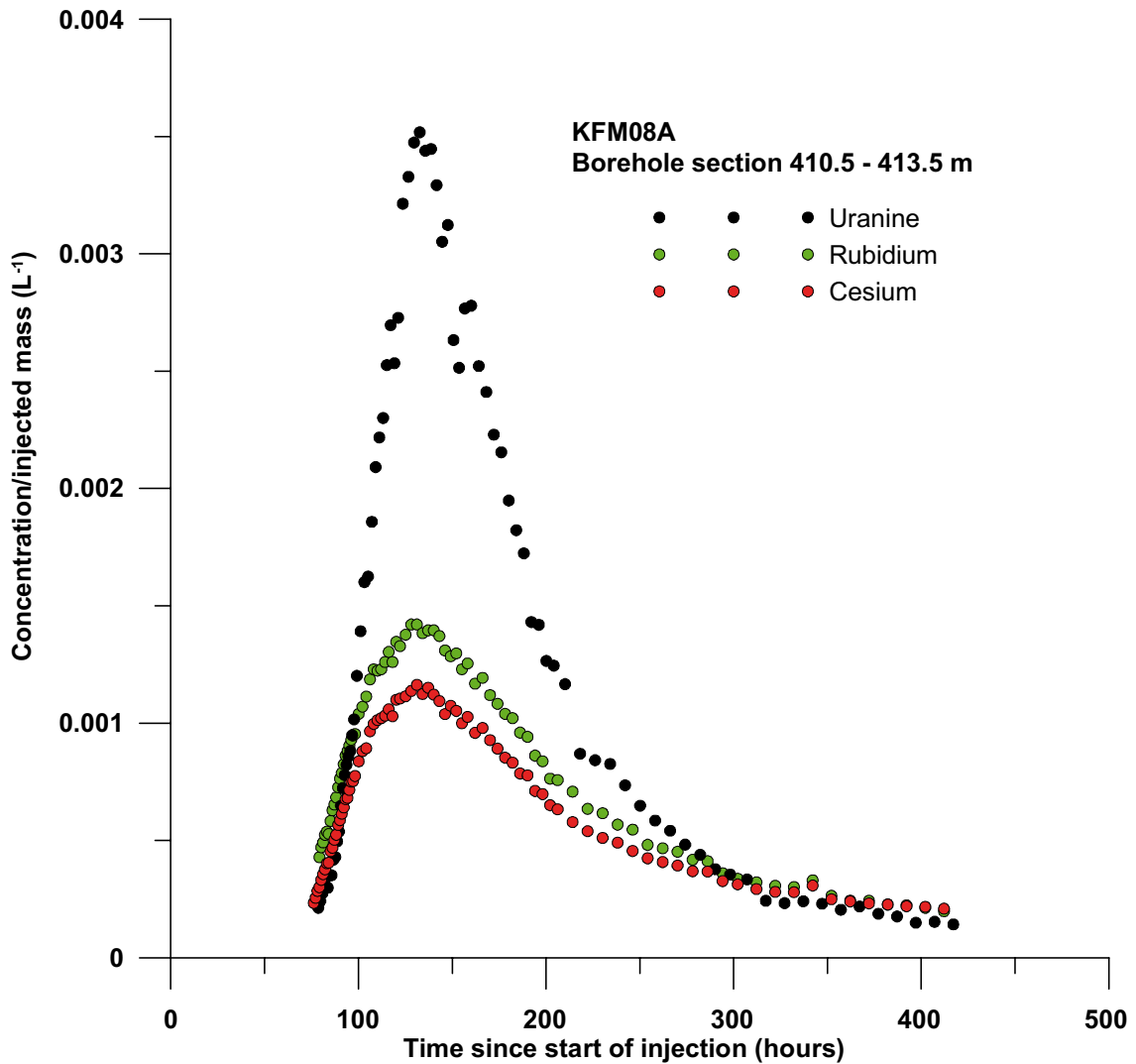


Figure 5-19. Normalised withdrawal (recovery) phase breakthrough curves for Uranine, cesium and rubidium in section 410.5–413.5 m in borehole KFM08A.

5.2.3 Model evaluation KFM08, 410.5–413.5 m

The model simulations were carried out assuming negligible hydraulic background gradient, i.e. radial flow. The simulated times and flows for the various experimental phases are given in Table 5-2. In the simulation model, the flow zone is approximated by a 0.1 m thick fracture zone.

The experimental evaluation was carried out by simultaneous model fitting of Uranine and a sorbing tracer as outlined in Section 4.4. Thus, separate regression analyses were carried out for simultaneous fitting of Uranine/cesium and Uranine/rubidium, respectively.

In each regression run, estimation parameters were longitudinal dispersivity (α_L) and a linear retardation factor (R), while the porosity was given a fixed value. Regression was carried out for four different values of porosity: 0.005, 0.01, 0.02 and 0.05. For all cases, the fits between model and experimental data are similar. Examples of model fits are shown in Figure 5-20a and Figure 5-20b.

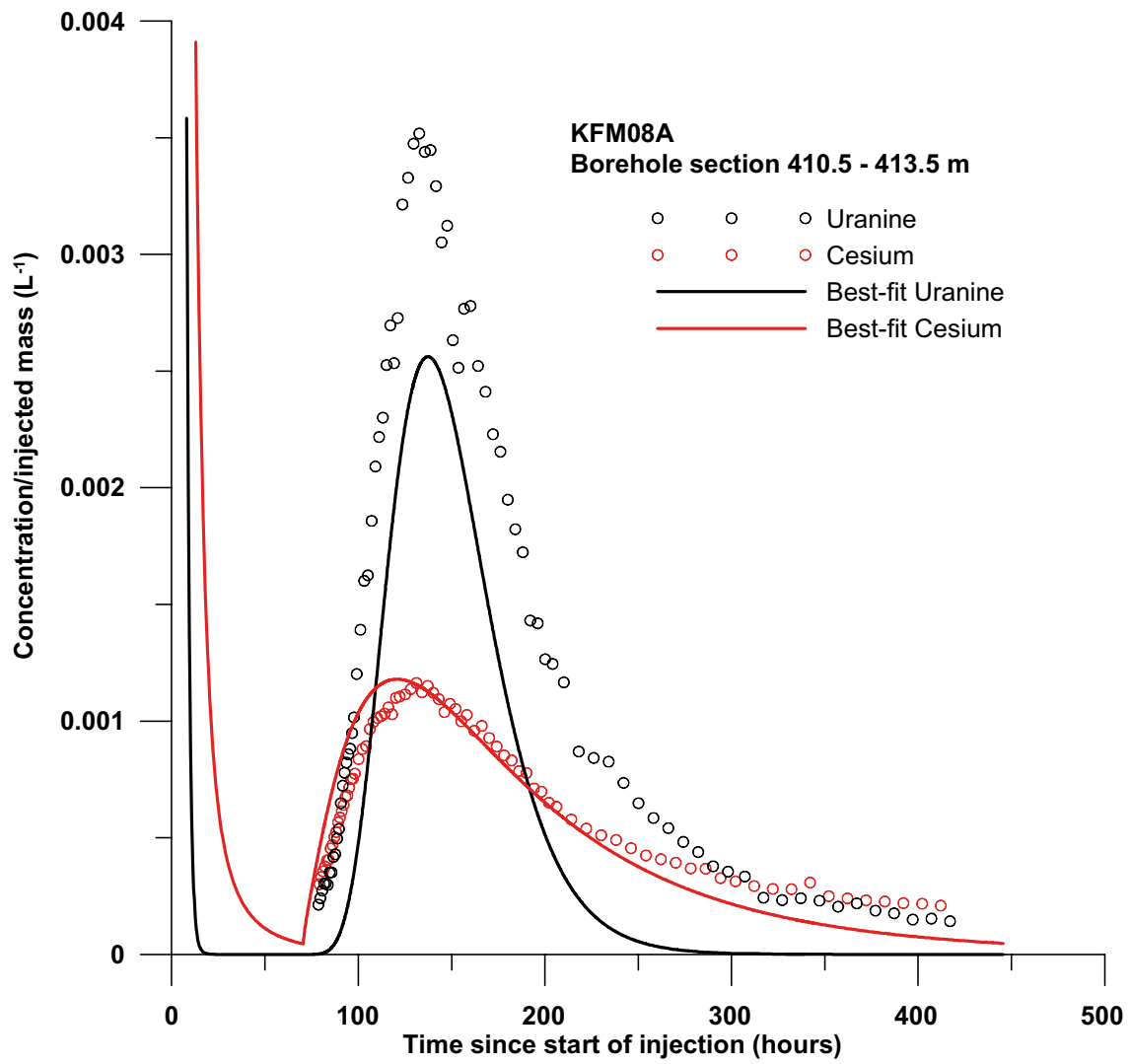


Figure 5-20a. Example of simultaneous fitting of Uranine and cesium for section 410.5–413.5 m in borehole KFM08A.

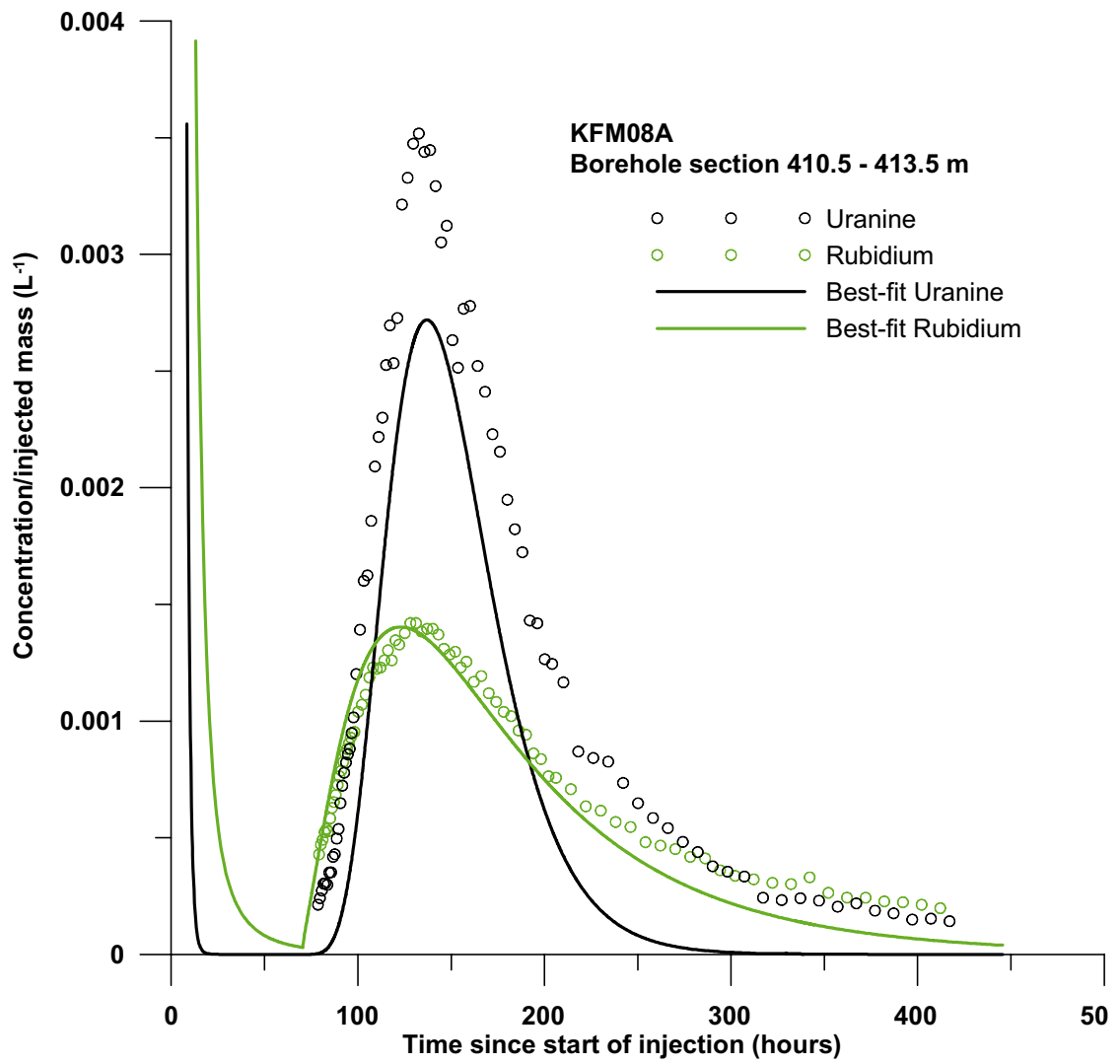


Figure 5-20b. Example of simultaneous fitting of Uranine and rubidium for section 410.5–413.5 m in borehole KFM08A.

The model fits to the experimental breakthrough curves are generally fairly good for the sorbing tracers (cesium and rubidium, respectively) but much less satisfactory for Uranine in either of the plots above. In addition to the, from previous SWIW experiments within the investigation programme, known problems when fitting the tail of the Uranine curve, the peak levels of the simulated Uranine curves are significantly below the observed ones. This inability to fit the peak of the Uranine curve has not been observed in evaluation of previously performed SWIW tests within the investigation programme.

Because the number of fitting parameters in this evaluation is very small, merely changing the parameter values will not provide a better fit. In fact, each regression run results in a fairly well-defined least-squares minimum. An example of what happens when Uranine data are assigned larger regression weights (i.e. the fit of the Uranine is given a high priority compared with the rubidium curve) is shown in Figure 5-21, where a regression run for simultaneous fitting of Uranine and rubidium is shown. In Figure 5-21, the Uranine curve fits much better (as would be expected) but the shape of the rubidium curve is clearly very different from the observed curve.

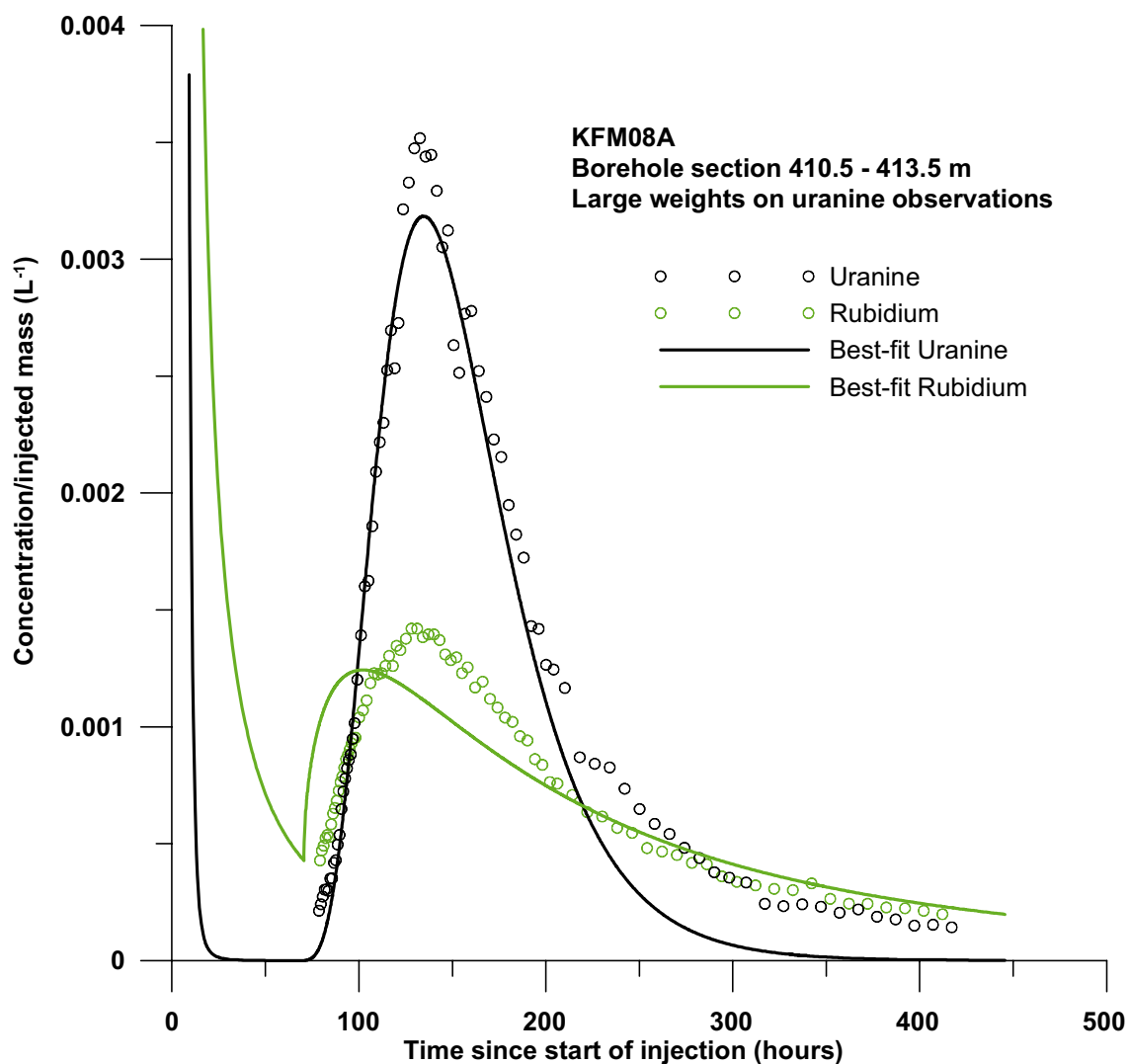


Figure 5-21. Example of model fit when Uranine data are assigned large regression weights.

Because the misfit of the Uranine curves mostly appears to be an inability to reach the peak level of the observed curve (the shape around the peak appears to conform fairly well to the Uranine data), one may make the hypothesis that the tracer recovery is not the same (as is assumed above) for all tracers. Thus, if tracer recovery for the sorbing tracers is lower than assumed, then the fit to the Uranine curve would be better. There are independent data that would indicate any difference in tracer recovery, but in the regression analysis this may be investigated by allowing an extra fitting parameter. A few regression runs were carried out (but not shown here) using this additional parameter, which resulted in fairly good fits for both tracers. However, by introducing this extra fitting parameter, much of the ability of this type of test to identify tracer retardation disappears. In other words, the determination of the retardation factor becomes much more ambiguous.

Another possibility that has been investigated to a fairly large extent is if there are errors in the experimental data. Although this investigation revealed a significant problem with the analysis for Uranine in some samples (see Section 4.5), it was concluded that there was no reason to expect that this error would have caused any errors in the C/M_{inj} values for Uranine.

Despite the inability to fit the peak of the Uranine curve, the simulations shown in Figure 5-20a and 5-20b were judged to be preferable compared with the alternatives discussed above.

All of the regression runs (Tables 5-3a and 5-3b) resulted in similar values of the retardation coefficient for each sorbing tracer, while the estimated values of the longitudinal dispersivity are strongly dependent on the assumed porosity value. Both of these observations are consistent with prior expectations of the relationships between parameters in a SWIW test /Nordqvist and Gustafsson 2002, 2004/ and /Gustafsson and Nordqvist 2005/.

The estimated values of R for cesium (33–36) and rubidium (19–24) indicate relatively strong sorption effects, although the estimated values are somewhat lower compared with previous SWIW tests as well as earlier cross-hole tests. For example, /Winberg et al. 2000/ reported a value for cesium of $R = 69$, while a value of $R = 140$ was reported by /Andersson et al. 1999/. Estimated values of R for rubidium are lower than for cesium, although one may consider the values being of similar magnitudes. This is somewhat contrary to literature data from the TRUE Block Scale Project /Anderson et al. 2002/, which indicate about one order of magnitude lower values of R for rubidium than for cesium. On the other hand, the precedent SWIW test in KLX03 /Gustafsson et al. 2006/, which so far is the only other SWIW tests within the site investigation programme where these three tracers have been used, resulted in more or less the same retardation factor for cesium and rubidium, respectively.

Table 5-3a. Results of simultaneous fitting of Uranine and cesium for section 410.5–413.5 m in borehole KFM08A. Approximate values of the coefficient of variation (estimation standard error divided by the estimated value) are given within parenthesis.

Porosity (fixed)	aL (estimated)	R (estimated)
0.005	0.29 (0.15)	35.7 (0.51)
0.01	0.20 (0.15)	34.4 (0.51)
0.02	0.14 (0.15)	35.9 (0.51)
0.05	0.09 (0.15)	33.4 (0.50)

Table 5-3b. Results of simultaneous fitting of Uranine and rubidium for section 410.5–413.5 m in borehole KFM08A. Approximate values of the coefficient of variation (estimation standard error divided by the estimated value) are given within parenthesis.

Porosity (fixed)	aL (estimated)	R (estimated)
0.005	0.33 (0.13)	19.3 (0.44)
0.01	0.23 (0.13)	20.4 (0.44)
0.02	0.16 (0.13)	20.8 (0.44)
0.05	0.09 (0.13)	23.5 (0.44)

6 Discussion and conclusions

The dilution measurements were carried out in selected fractures and fracture zones in borehole KFM08A (inclination from -60 at collar to -36 at 1,000 m) at levels from 188 to 685 m borehole length (elevation -160 to -550 m), where hydraulic transmissivity ranged within $T = 1.1 \cdot 10^{-8}$ – $2.2 \cdot 10^{-6}$ m²/s. The borehole intersects with the deformation zones that are identified by SKB's single hole interpretation (SHI) of cored boreholes as seen in Figure 6-1, and as modelled in SDM version 2.1, Table 6-1.

The results of the dilution measurements in borehole KFM08A show that the groundwater flow varies considerably during natural, i.e. undisturbed conditions, with flow rates from 0.03 to 2.21 ml/min and Darcy velocities from $9.3 \cdot 10^{-10}$ to $8.0 \cdot 10^{-8}$ m/s ($8.0 \cdot 10^{-5}$ – $6.9 \cdot 10^{-3}$ m/d). These results are in accordance with dilution measurements carried out in boreholes KFM01A, KFM02A, KFM03A and KFM03B. In these boreholes hydraulic transmissivity in the test sections was within $T = 2.7 \cdot 10^{-10}$ – $9.2 \cdot 10^{-5}$ m²/s and flow rate ranged from 0.01 to 23.3 ml/min and Darcy velocity from $7.8 \cdot 10^{-10}$ to $8.4 \cdot 10^{-7}$ m/s ($6.7 \cdot 10^{-5}$ – $7.3 \cdot 10^{-2}$ m/d) /Gustafsson et al. 2005/. Groundwater flow rates and Darcy velocities calculated from dilution measurements in borehole KFM08A are also within the range that can be expected out of experience from previously performed dilution measurements under natural gradient conditions at other sites in Swedish crystalline rock /Gustafsson and Andersson 1991, Gustafsson and Morosini 2002, Gustafsson and Nordqvist 2005, Gustafsson et al. 2006/.

The general trend in KFM08A, as in most other measured boreholes, is that the Darcy velocity and the flow rate decrease with depth. The only exception is the section at c. 685 m borehole length, where the flow is high in spite of the depth. The high flow rate may be explained by a high hydraulic transmissivity in combination with a hydraulic shortcut where the measured fracture constitutes a hydraulic conductor between other fractures with different hydraulic heads. It may also be considered that in fractured rock, during natural hydraulic conditions, the groundwater flow in fractures and fracture zones to a large extent is governed by the direction of the large-scale hydraulic gradient relative to the strike and dip of the conductive fractures and zones.

A large portion of the measured fractures/fracture zones are within a small range of transmissivity. However it is indicated that groundwater flow rate is proportional to hydraulic transmissivity.

Hydraulic gradients, calculated according to the Darcy concept, are within the expected range (0.001–0.05) in three out of five measured test sections. In the single fracture section at c. 188 m and in the minor fracture zone at c. 410 m borehole length the hydraulic gradient is considered very large. Local effects where the measured fractures constitutes a hydraulic conductor between other fractures with different hydraulic heads or wrong estimations of the correction factor, α , and/or the hydraulic conductivity of the fracture could explain the large hydraulic gradients. The pressure decrease at the beginning of the measurement at c. 410 m may give some contribution to the measured groundwater flow rate and hence to the large calculated hydraulic gradient. The hydraulic transmissivity of the section is also at the lower limit of measurement range for the dilution probe which may decrease accuracy in determined groundwater flow rate.

The SWIW experiment in the borehole section at 410.5–413.5 m borehole length resulted in high quality tracer breakthrough data. Experimental conditions (flows, times, events, etc) are well known and documented, which provides a good basis for further evaluation of the data.

The results show smooth breakthrough curves without apparent irregularities or excessive experimental noise with a clearly visible effect of retardation/sorption of cesium and rubidium.

The model evaluation was made using a radial flow model with advection, dispersion and linear equilibrium sorption as transport processes. It is important that experimental conditions (times, flows, injection concentration, etc) are incorporated accurately. Otherwise artefacts of erroneous input may occur in the simulated results. The evaluation carried out may be regarded as a typical preliminary approach for evaluation of a SWIW test where sorbing tracers are used. Background flow was in this case assumed to be insignificant.

The estimated values of the retardation factor for cesium (about 33–36) and rubidium (about 19–24) indicate relatively strong retardation/sorption, although these values are much lower (about one order of magnitude) than for the preceding SWIW test in KLX03 /Gustafsson et al. 2006/.

It should also be pointed out that the lack of model fit in the tailing parts of the curves in addition to lack of fit for the Uranine peak, appears to be a consistent feature in the SWIW tests performed so far /Gustafsson and Nordqvist 2005, Gustafsson et al. 2005, 2006/. Thus, there seems to be some generally occurring process that has not yet been identified, but is currently believed to be an effect of the tested medium and not an experimental artefact. Studies to identify possible causes for the observed discrepancy are ongoing.

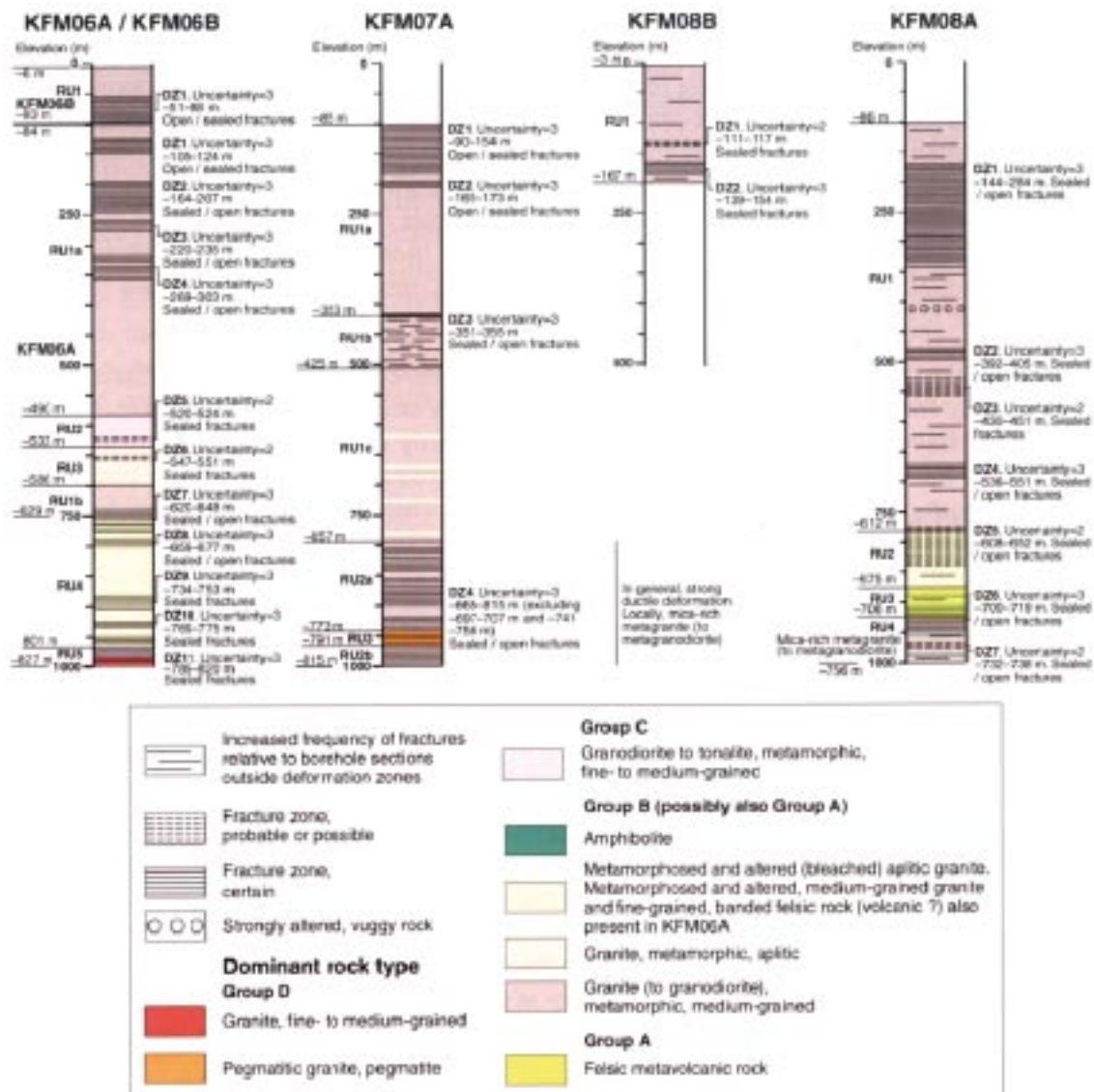


Figure 6-1. Rock units and possible deformation zones based on the single hole interpretations of the cored boreholes analysed for the first time during SDM version 2.1. (From /SKB 2006/, Figure 2-15).

Table 6-1. Intersected zones, Groundwater flows, Darcy velocities and Hydraulic gradients for all measured sections in boreholes KFM08A.

Borehole	Test section (m)	Intersected zones**	Noof flowing fractures*	T (m ² /s)*	Q (ml/min)	Q (m ³ /s)	Darcy velocity (m/s)	Hydraulic gradient
KFM08A	188.5–191.5		1	2.20E–06	2.21	3.7E–08	8.9E–08	0.11
KFM08A	274.5–277.5	ZFMNE1061	3–4	1.29E–06	0.39	6.5E–09	1.4E–08	0.033
KFM08A	410.5–413.5		3	1.13E–08	0.10	1.6E–09	3.6E–09	0.95
KFM08A	479.0–482.0	ZFMNS1204	1–2	6.93E–08	0.026	4.3E–10	9.3E–10	0.040
KFM08A	685.5–688.5		1	1.41E–06	0.25	4.2E–09	9.1E–09	0.019

* /Sokolnicki and Rouhiainen 2005/.

** /SKB 2006/.

7 References

- Andersson P, 1995.** Compilation of tracer tests in fractured rock. SKB PR 25-95-05, Svensk Kärnbränslehantering AB.
- Andersson P, Byegård J, Winberg A, 2002.** Final report of the TRUE Block Scale project. 2. Tracer tests in the block scale. SKB TR-02-14, Svensk Kärnbränslehantering AB.
- Andersson P, Wass E, Byegård J, Johansson H, Skarnemark G, 1999.** Äspö Hard Rock Laboratory. True 1st stage tracer programme. Tracer test with sorbing tracers. Experimental description and preliminary evaluation. SKB IPR-99-15, Svensk Kärnbränslehantering AB.
- Byegård J, Tullborg E-L, 2005.** Sorption experiments and leaching studies using fault gouge material and rim zone material from the Äspö Hard Rock Laboratory. SKB Technical Report (in prep.), Svensk Kärnbränslehantering AB.
- Gustafsson E, 2002.** Bestämning av grundvattenflödet med utspädningsteknik – Modifiering av utrustning och kompletterande mätningar. SKB R-02-31 (in Swedish), Svensk Kärnbränslehantering AB.
- Gustafsson E, Andersson P, 1991.** Groundwater flow conditions in a low-angle fracture zone at Finnsjön, Sweden. *Journal of Hydrology*, Vol 126, pp 79–111. Elsevier, Amsterdam.
- Gustafsson E, Morosini M, 2002.** In-situ groundwater flow measurements as a tool for hardrock site characterisation within the SKB programme. *Norges geologiske undersøkelse. Bulletin 439*, 33–44.
- Gustafsson E, Nordqvist R, 2005.** Oskarshamn site investigation. Groundwater flow measurements and SWIW-tests in boreholes KLX02 and KSH02. SKB P-05-28, Svensk Kärnbränslehantering AB.
- Gustafsson E, Nordqvist R, Thur P, 2005.** Forsmark site investigation. Groundwater flow measurements and SWIW tests in boreholes KFM01A, KFM02A, KFM03A and KFM03B. SKB P-05-77, Svensk Kärnbränslehantering AB.
- Gustafsson E, Nordqvist R, Thur P, 2006.** Oskarshamn site investigation. Groundwater flow measurements and SWIW-tests in borehole KLX03. SKB P-05-246, Svensk Kärnbränslehantering AB.
- Halevy E, Moser H, Zellhofer O, Zuber A, 1967.** Borehole dilution techniques – a critical review. In: *Isotopes in Hydrology, Proceedings of a Symposium, Vienna 1967*, IAEA, Vienna, pp 530–564.
- Nordqvist R, Gustafsson E, 2002.** Single-well injection-withdrawal tests (SWIW). Literature review and scoping calculations for homogeneous crystalline bedrock conditions. SKB R-02-34, Svensk Kärnbränslehantering AB.
- Nordqvist R, Gustafsson E, 2004.** Single-well injection-withdrawal tests (SWIW). Investigation of evaluation aspects under heterogeneous crystalline bedrock conditions. SKB R-04-57, Svensk Kärnbränslehantering AB.
- Rhén I, Forsmark T, Gustafson G, 1991.** Transformation of dilution rates in borehole sections to groundwater flow in the bedrock. Technical note 30. In: Liedholm M. (ed) 1991. SKB-Äspö Hard Rock Laboratory, Conceptual Modeling of Äspö, technical Notes 13–32. General Geological, Hydrogeological and Hydrochemical information. Äspö Hard Rock Laboratory Progress Report PR 25-90-16b.

SKB, 2001a. Program för platsundersökning vid Forsmark. SKB R-01-42 (in Swedish), Svensk Kärnbränslehantering AB.

SKB, 2001b. Site investigations – Investigation methods and general execution programme. SKB TR-01-29, Svensk Kärnbränslehantering AB.

SKB, 2006. Site modelling Forsmark step 2.1. SKB R-06-38, Svensk Kärnbränslehantering AB.

Sokolnicki M, Rouhiainen P, 2005. Forsmark site investigation. Difference flow logging in borehole KFM08A. SKB P-05-43, Svensk Kärnbränslehantering AB.

Winberg A, Andersson P, Hermansson J, Byegård J, Cvetkovic V, Birgersson L, 2000. Äspö Hard Rock Laboratory. Final report of the first stage of the tracer retention understanding experiment. SKB TR-00-07, Svensk Kärnbränslehantering AB.

Voss C I, 1984. SUTRA – Saturated-Unsaturated Transport. A finite element simulation model for saturated-unsaturated fluid-density-dependent ground-water flow with energy transport or chemically-reactive single-species solute transport. U.S. Geological Survey Water-Resources Investigations Report 84-4369.

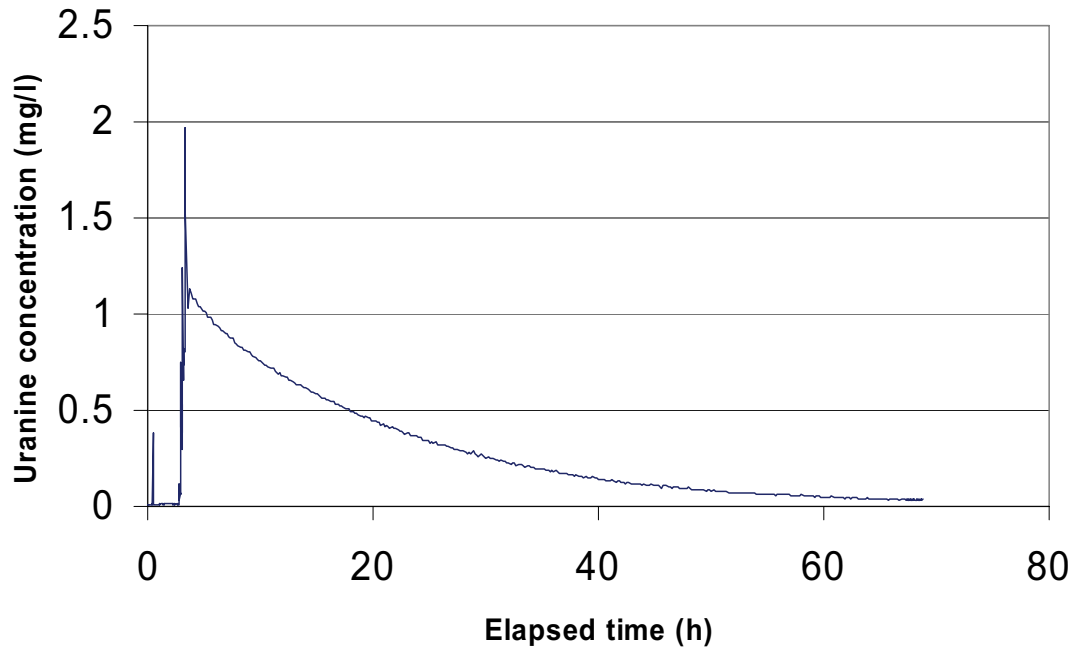
Borehole data KFM08A

SICADA – Information about KFM08A

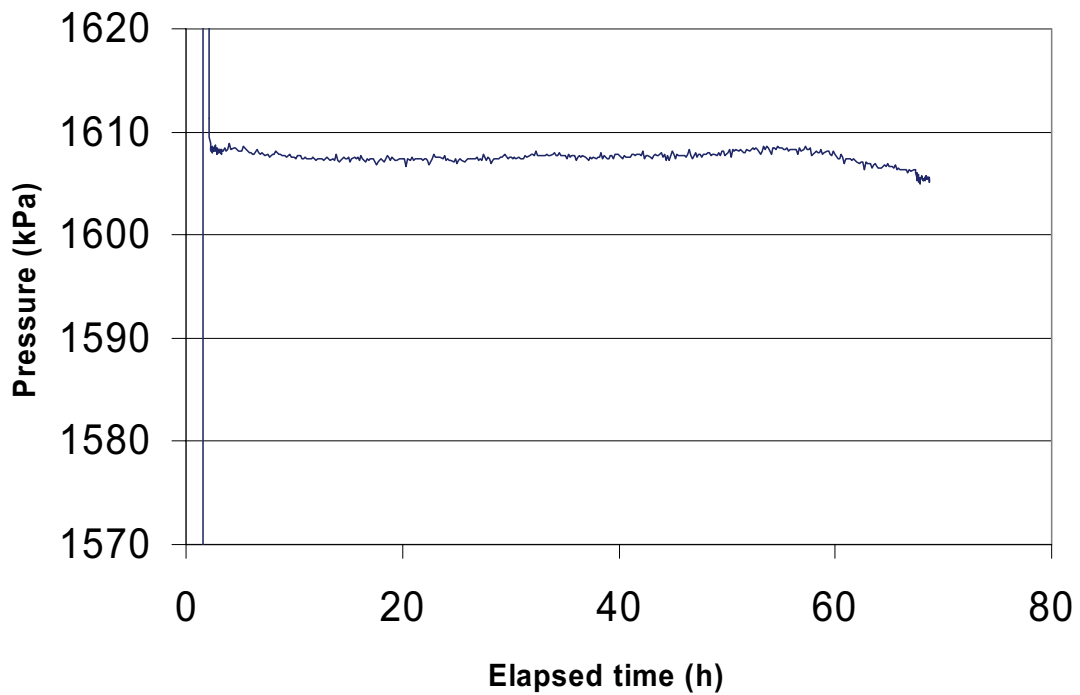
Title	Value				
	Information about cored borehole KFM08A (2005-12-09),				
Comment:	No comment exist				
Borehole length (m):	1,001.190				
Reference level:	Rostfri flans (Flange at Top of Casing)				
Drilling Period (s):	<i>From Date</i>	<i>To Date</i>	<i>Secup(m)</i>	<i>Seclow(m)</i>	<i>Drilling Type</i>
	2004-09-13	2004-09-27	0.00	100.450	Percussion drilling
	2005-01-25	2005-01-25	97.140	100.550	Core drilling
	2005-01-25	2005-03-31	100.550	1,000.190	Core drilling
Starting point coordinate:	<i>Length (m)</i>	<i>Northing (m)</i>	<i>Easting (m)</i>	<i>Elevation</i>	<i>Coord System</i>
	0.000	6700494.492	1631197.060	2.487	RT90-RHB70
	3.000	6700495.626	1631196.141	-0.134	RT90-RHB70
Angles:	<i>Length (m)</i>	<i>Bearing</i>	<i>Inclination (- = down)</i>	<i>Coord System</i>	
	0.000	321.000	-60.887	RT90-RHB70	
Borehole diameter:	<i>Secup (m)</i>	<i>Seclow (m)</i>	<i>Hole Diam (m)</i>		
	0.000	9.140	0.343		
	9.140	97.140	0.249		
	97.140	102.400	0.086		
	102.400	1,001.190	0.077		
Casing diameter:	<i>Secup (m)</i>	<i>Seclow (m)</i>	<i>Case In (m)</i>	<i>Case Out(m)</i>	
	0.000	100.150	0.200	0.208	
	0.230	9.140	0.310	0.323	
	100.150	100.200	0.170	0.208	
Cone dimensions:	<i>Secup (m)</i>	<i>Seclow (m)</i>	<i>Cone In (m)</i>	<i>Cone Out(m)</i>	
	94.080	102.260	0.080	0.195	
Grove milling:	<i>Length (m)</i>	<i>Tracer detectable</i>			
	151.000	Ja			
	200.000	Ja			
	250.000	Ja			
	299.800	Ja			
	350.000	Ja			
	400.000	Ja			
	450.000	Ja			
	500.000	Ja			
	552.000	Ja			
	600.000	Ja			
	650.000	Ja			
	700.000	Ja			
	750.000	Ja			
	800.000	Ja			
	850.000	Ja			
	900.000	Ja			
	950.000	Ja			
	981.000	Ja			

Dilution measurement KFM08A 188.5–191.5 m

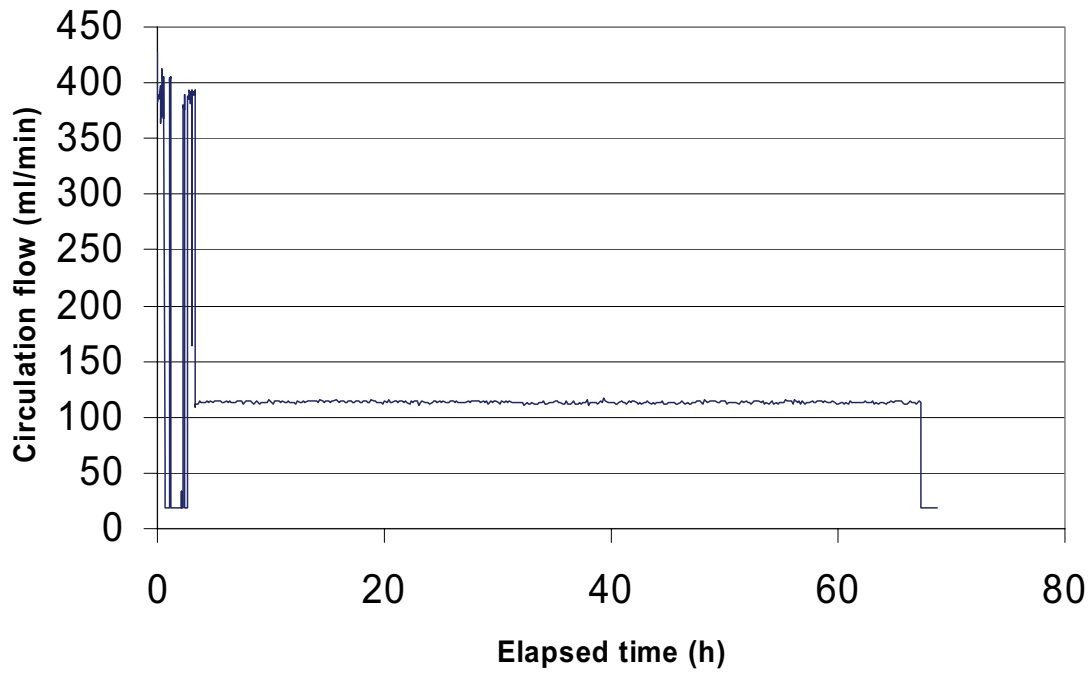
KFM08A 188.5-191.5 m



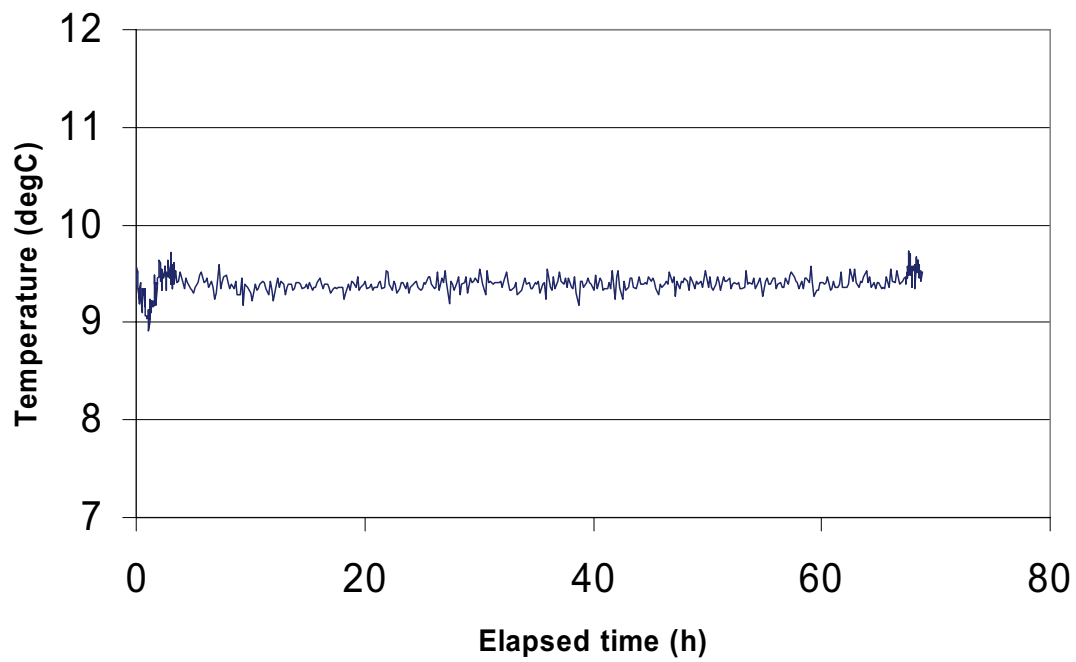
KFM08A 188.5-191.5 m



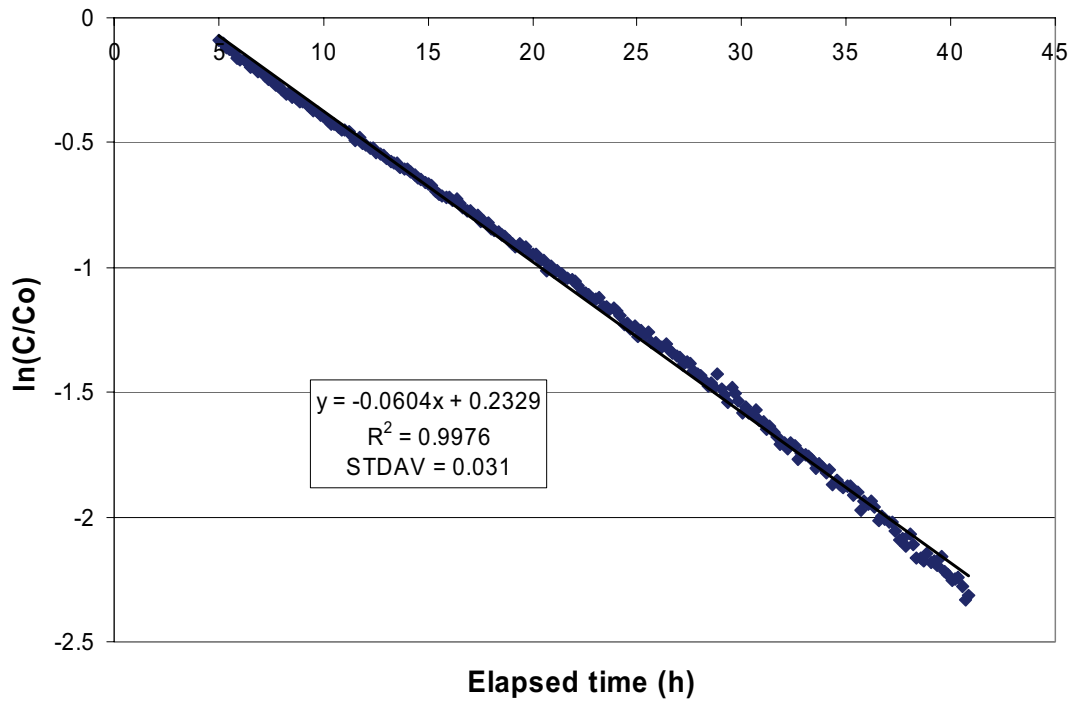
KFM08A 188.5-191.5 m



KFM08A 188.5-191.5 m



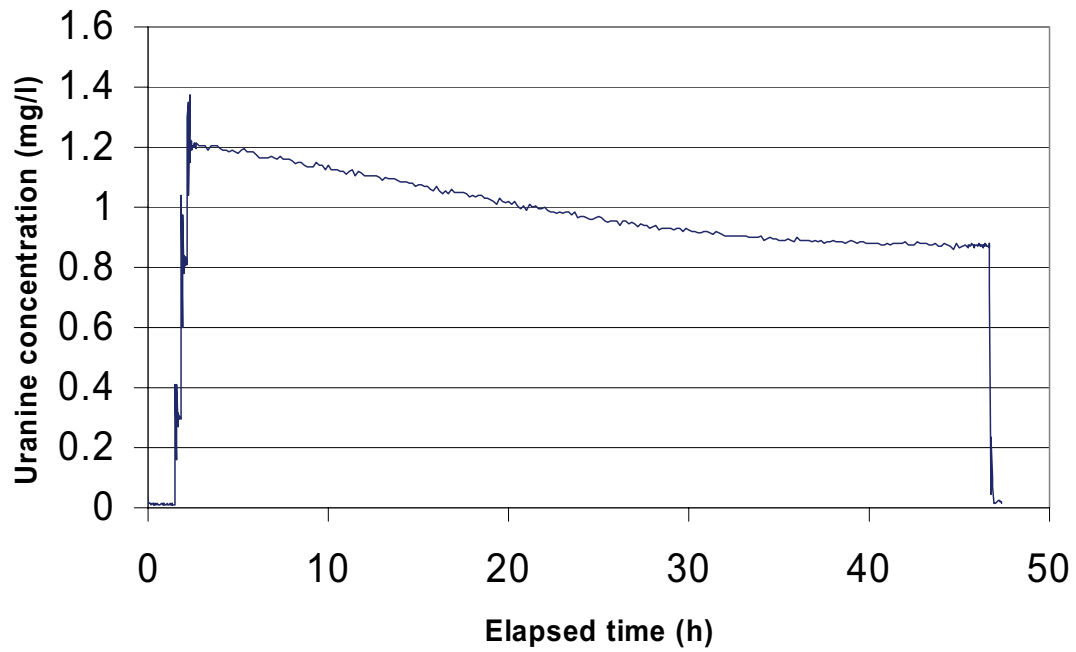
KFM08A 188.5-191.5 m



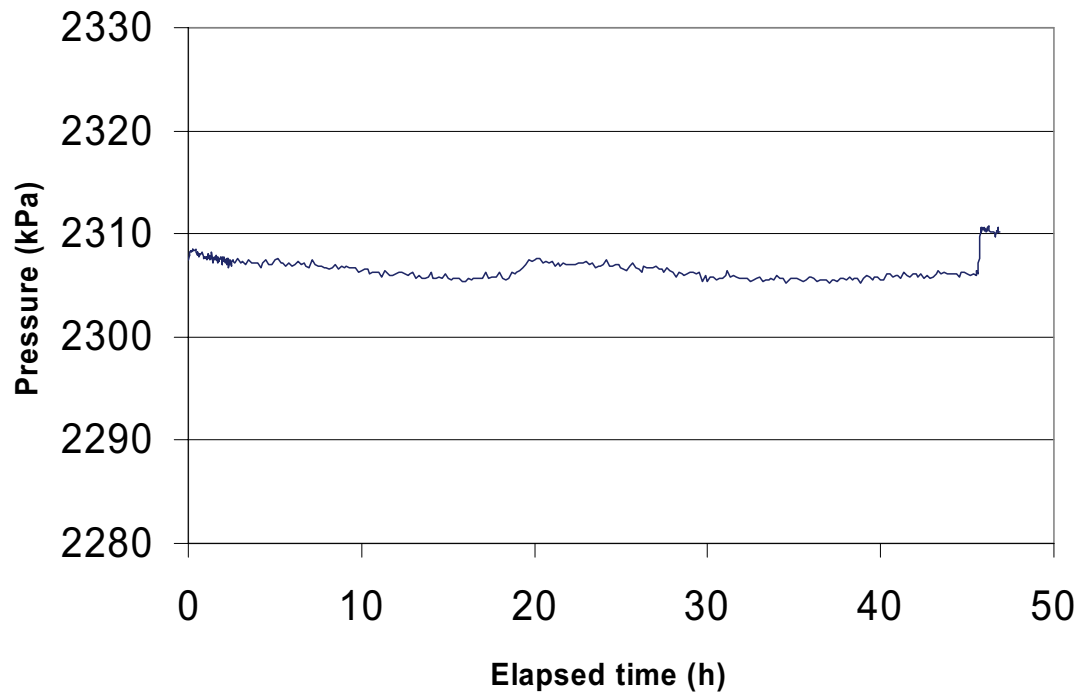
Part of dilution curve	V (ml)	ln(C/Co)/t	Q (ml/h)	Q (ml/min)	Q (m ³ /s)	R-2value
5-40	2,200	-0.0604	132.88	2.215	369E-08	0.9976
Part of dilution curve	K (m/s)	Q (m ³ /s)	A (m ²)	v (m/s)	l	
5-40	7.33E-07	3.69E-08	0.4620	7.99E-08	0.109	

Dilution measurement KFM08A 274.5–277.5 m

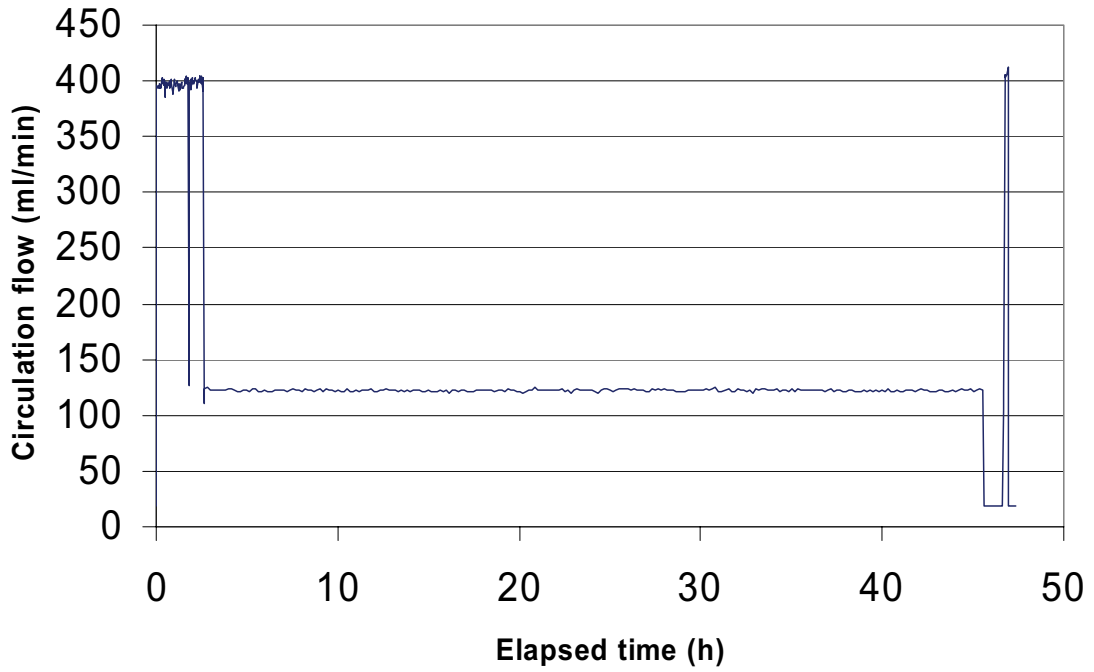
KFM08A 274.5-277.5 m



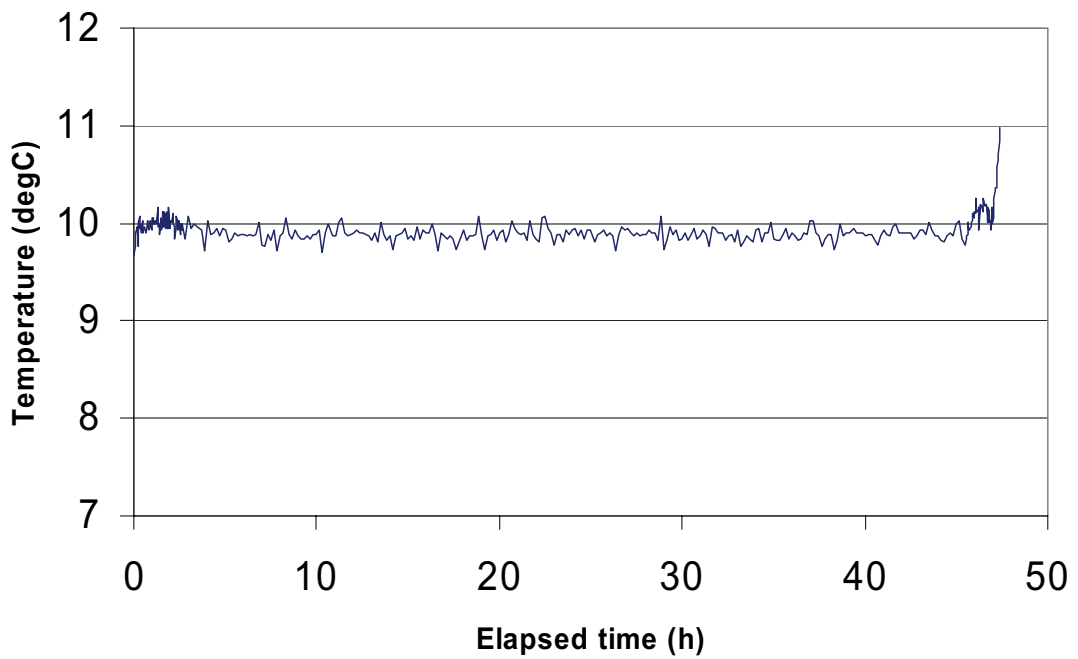
KFM08A 274.5-277.5 m



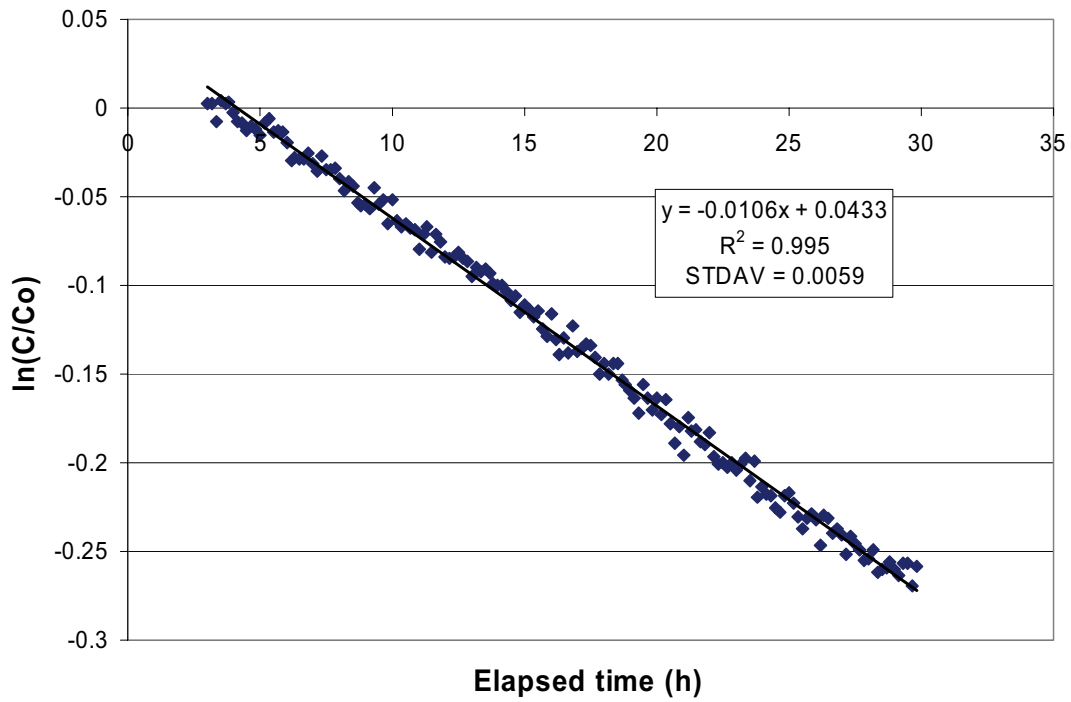
KFM08A 274.5-277.5 m



KFM08A 274.5-277.5 m



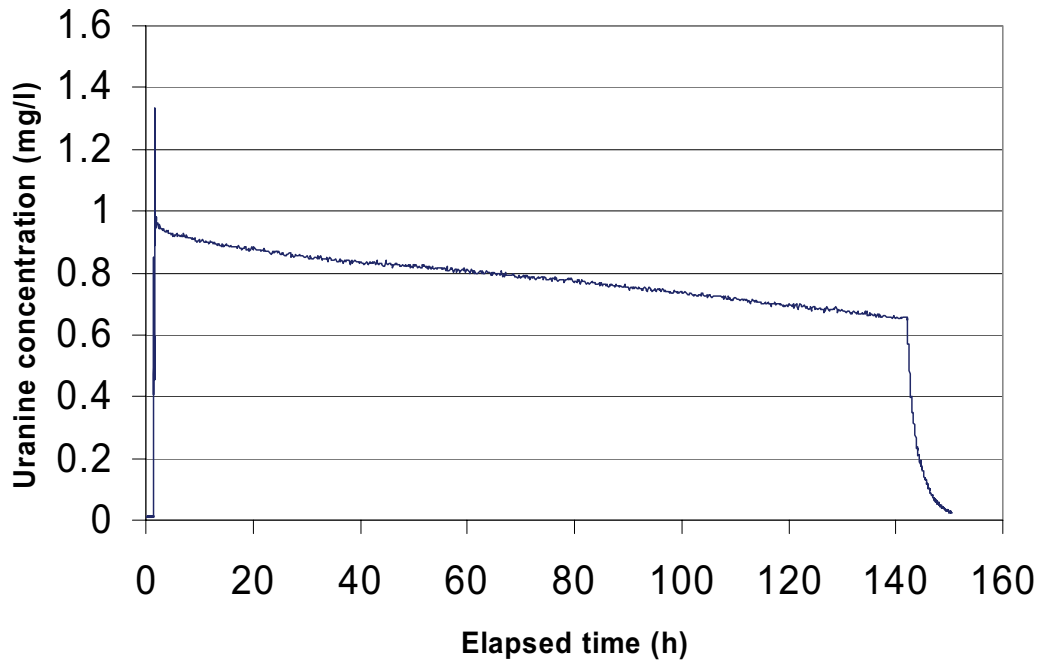
KFM08A 274.5-277.5 m



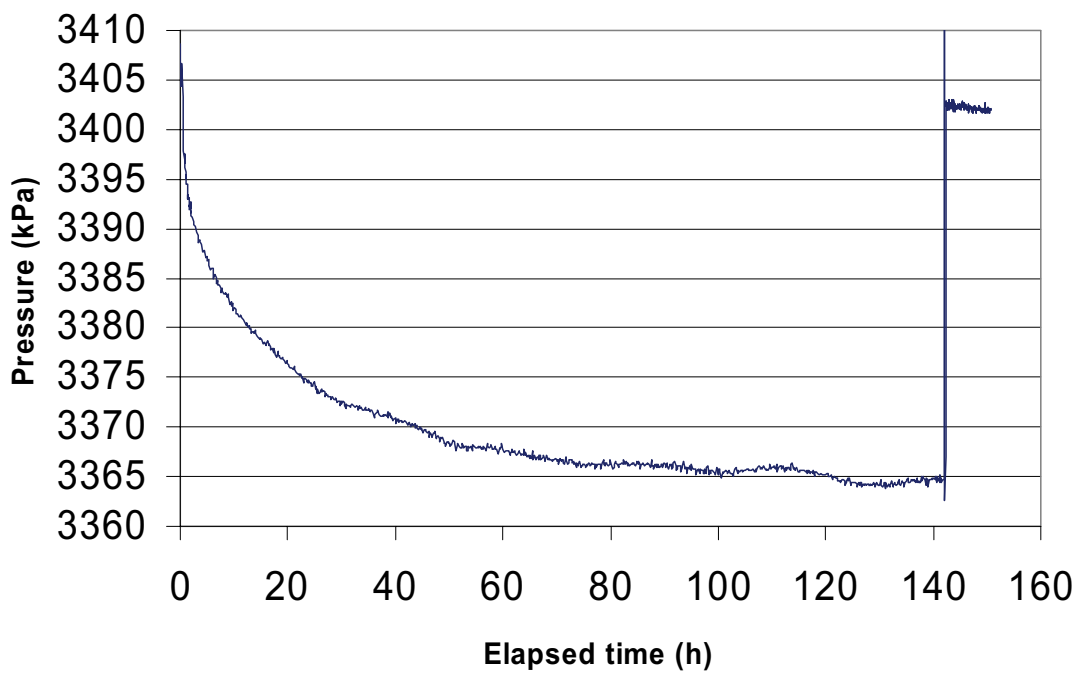
Part of dilution curve	V (ml)	ln(C/Co)/t	Q (ml/h)	Q (ml/min)	Q (m ³ /s)	R-2value
3~30	2,200	-0.0106	23.32	0.389	6.48E-09	0.9950
Part of dilution curve	K (m/s)	Q (m ³ /s)	A (m ²)	v (m/s)	I	
3~30	4.31E-07	6.48E-09	0.4620	1.40E-08	0.033	

Dilution measurement KFM01A 410.5–413.5 m

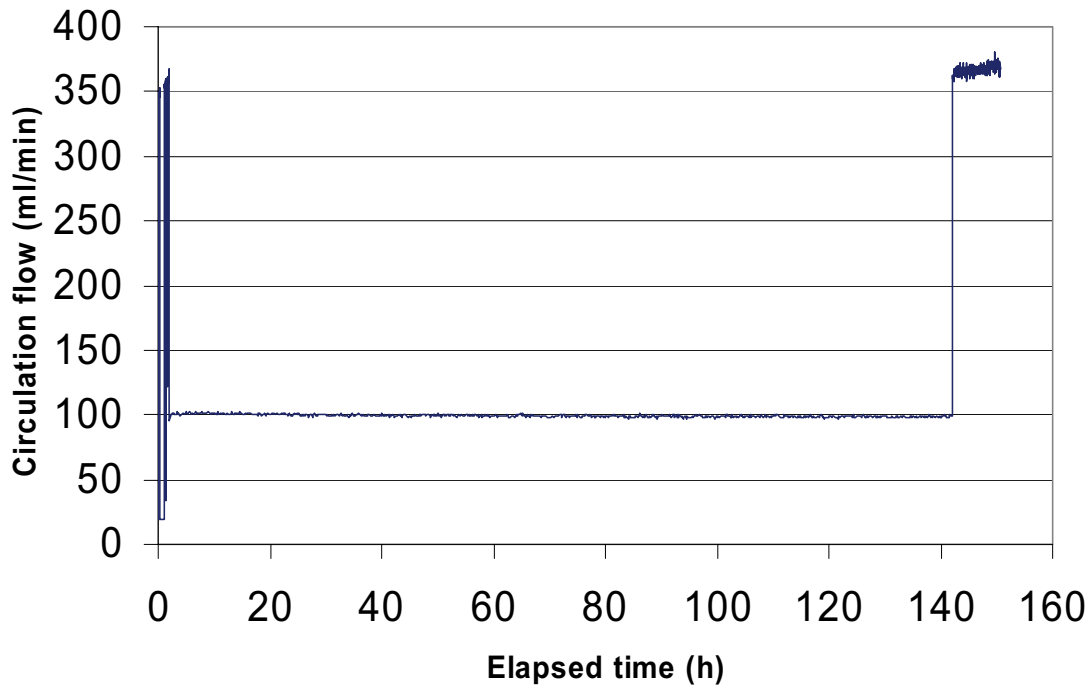
KFM08A 410.5 - 413.5 m



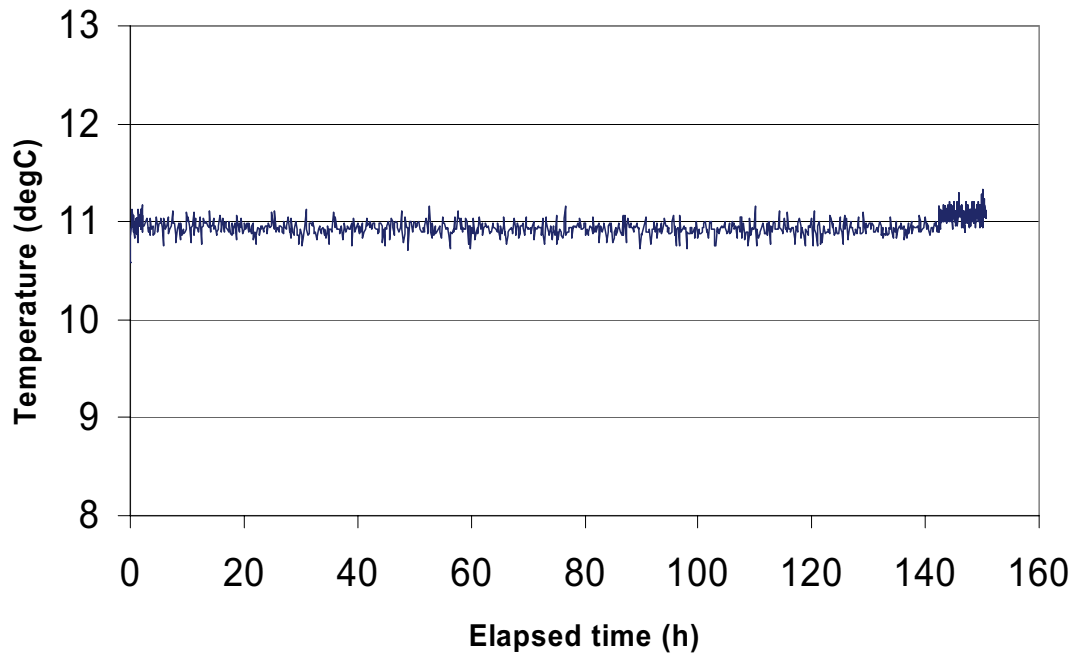
KFM08A 410.5 - 413.5 m



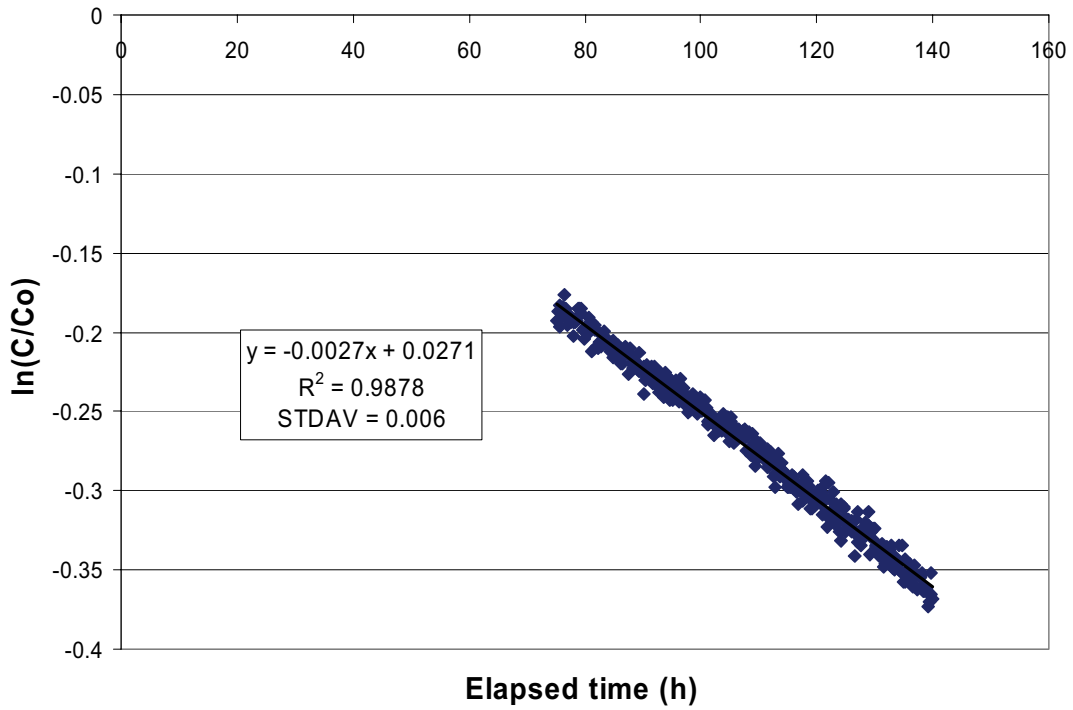
KFM08A 410.5 - 413.5 m



KFM08A 410.5 - 413.5 m



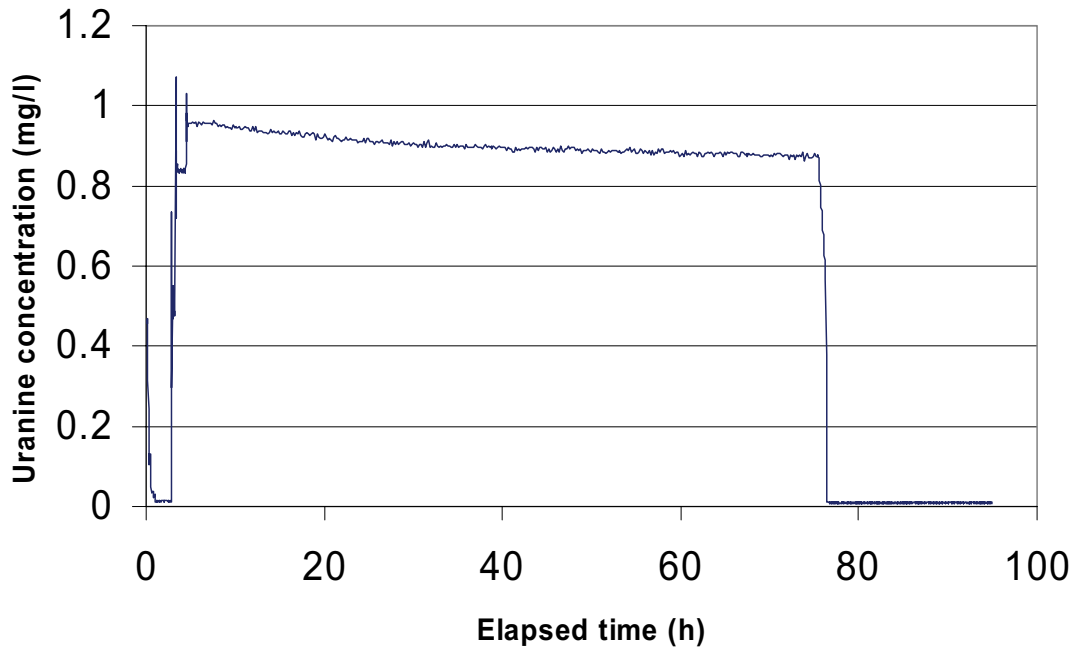
KFM08A 410.5 - 413.5 m



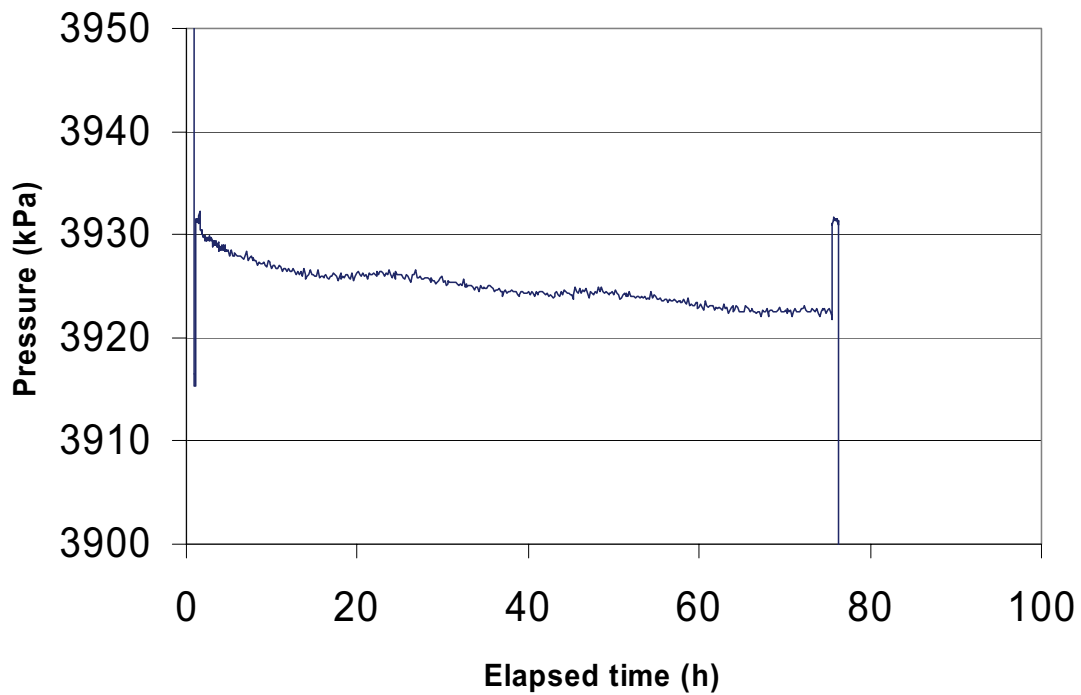
Part of dilution curve	V (ml)	ln(C/Co)/t	Q (ml/h)	Q (ml/min)	Q (m ³ /s)	R-2value
75-140	2,200	-0.0027	5.94	0.099	1.65E-09	0.9878
Part of dilution curve	K (m/s)	Q (m ³ /s)	A (m ²)	v (m/s)	l	
75-140	3.77E-09	1.65E-09	0.4620	3.57E-09	0.947	

Dilution measurement KFM02A 479.0–482.0 m

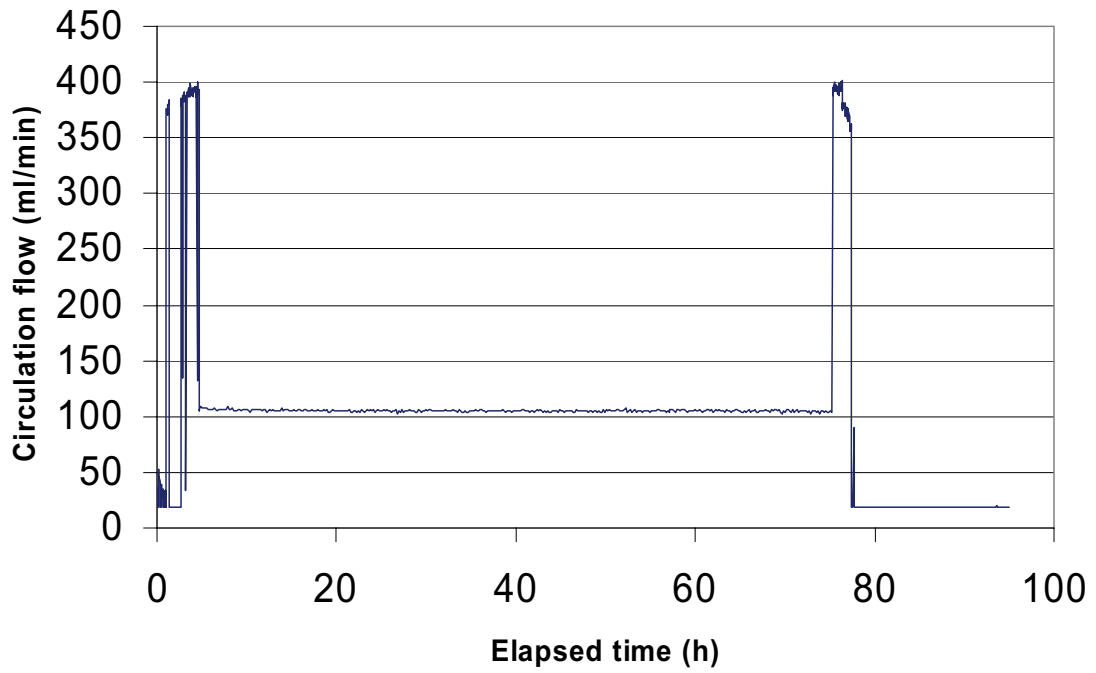
KFM08A 479.0-482.0 m



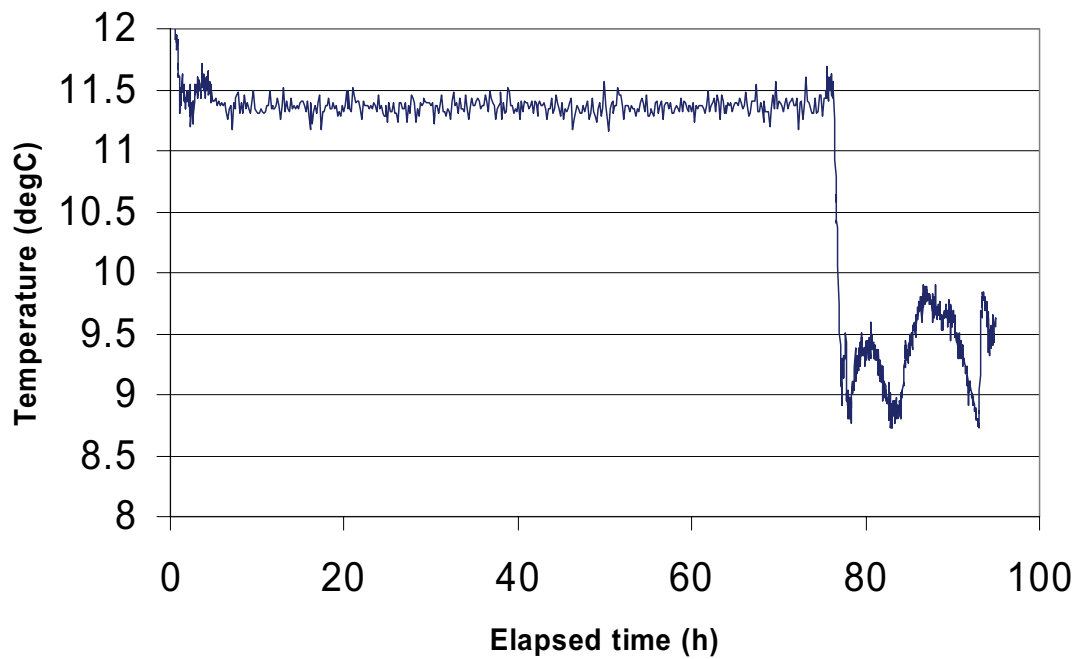
KFM08A 479.0-482.0 m



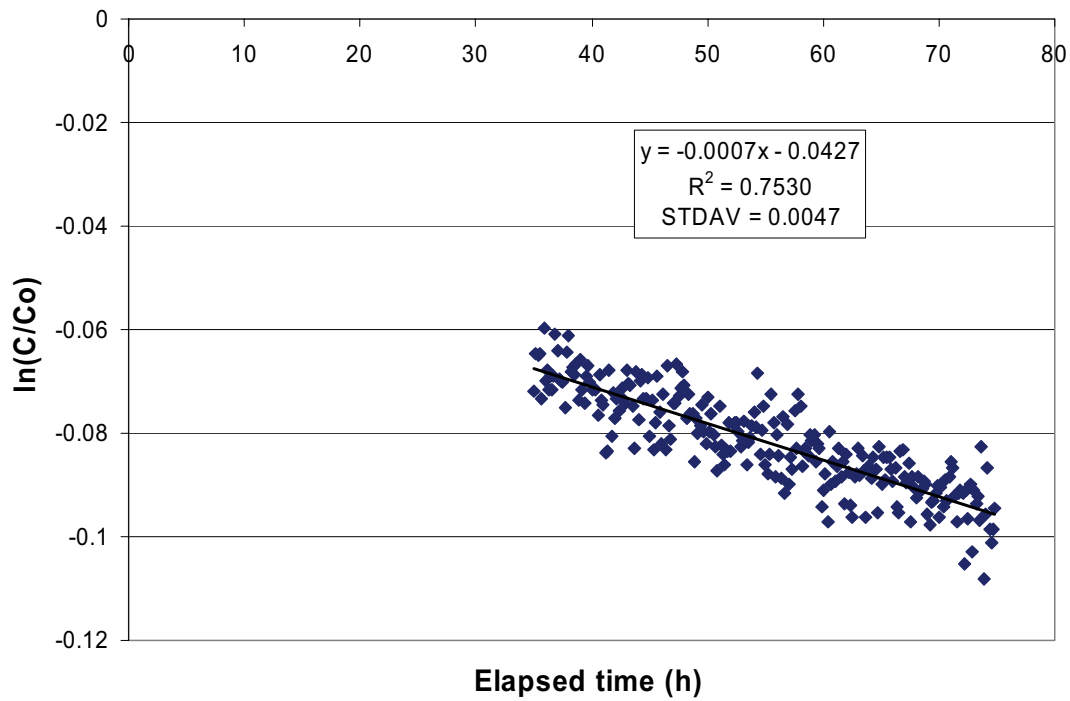
KFM08A 479.0-482.0 m



KFM08A 479.0-482.0 m



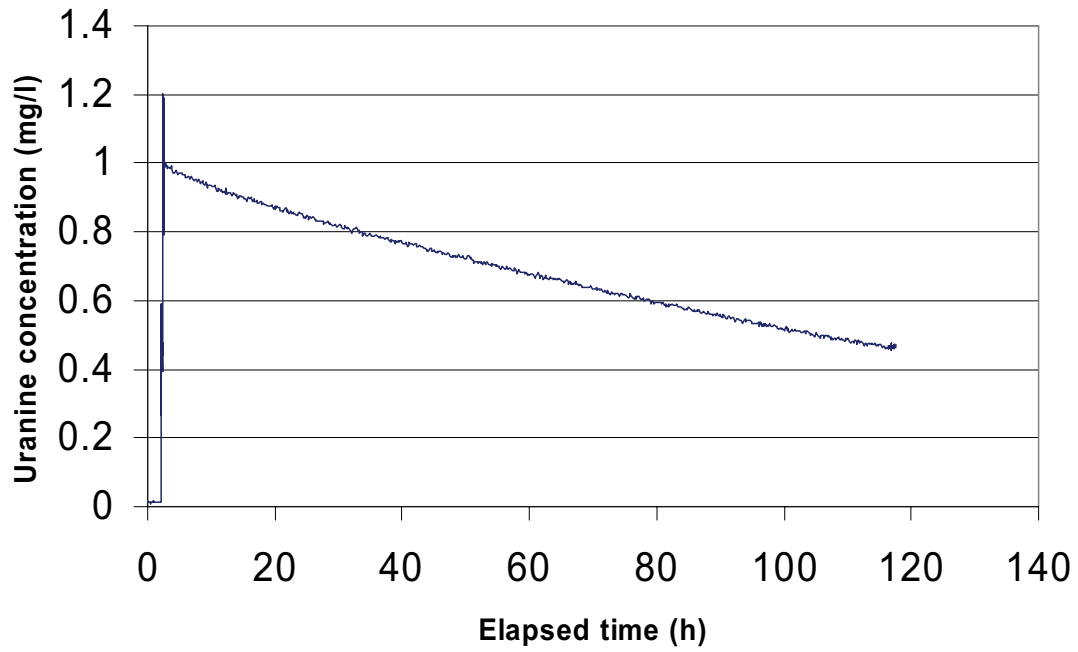
KFM08A 479.0-482.0 m



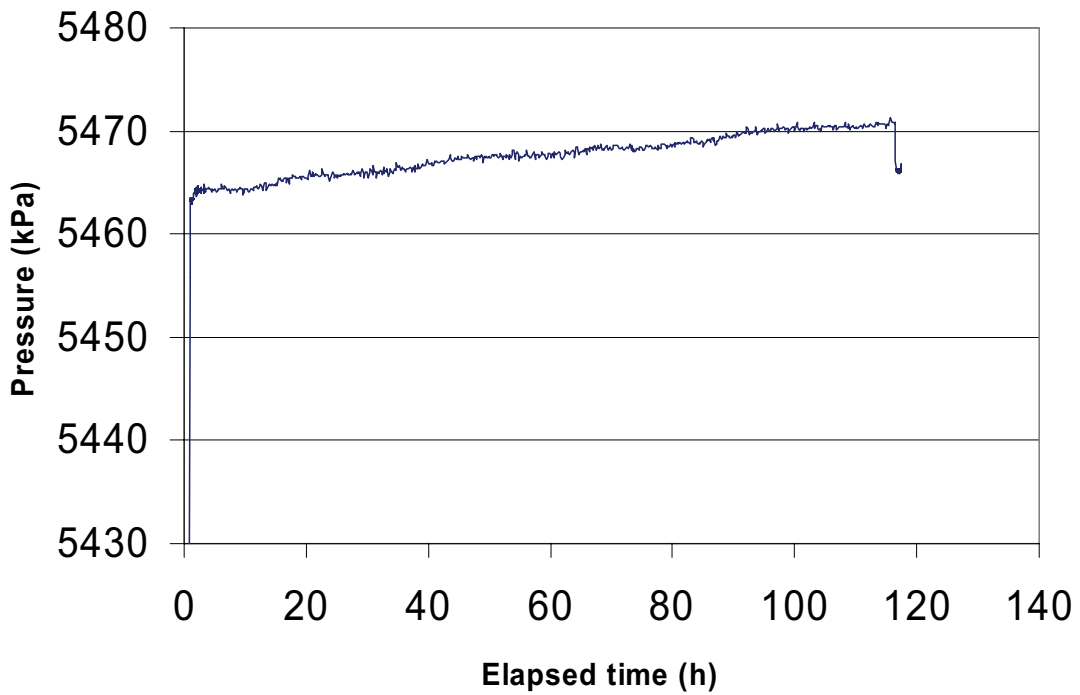
Part of dilution curve	V (ml)	ln(C/Co)/t	Q (ml/h)	Q (ml/min)	Q (m ³ /s)	R-2value
35-75	2,200	-0.0007	1.54	0.026	4.28E-10	0.7530
Part of dilution curve	K (m/s)	Q (m ³ /s)	A (m ²)	v (m/s)	I	
35-75	2.31E-08	4.28E-10	0.4620	9.26E-10	0.040	

Dilution measurement KFM02A 685.5–688.5 m

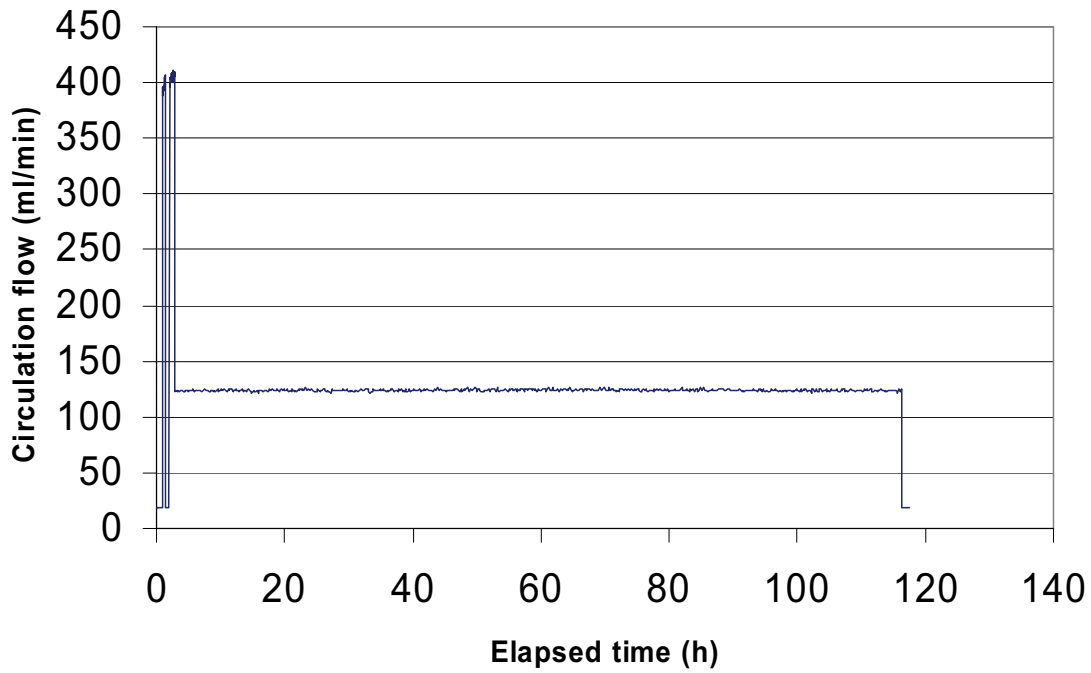
KFM08A 685.5 - 688.5 m



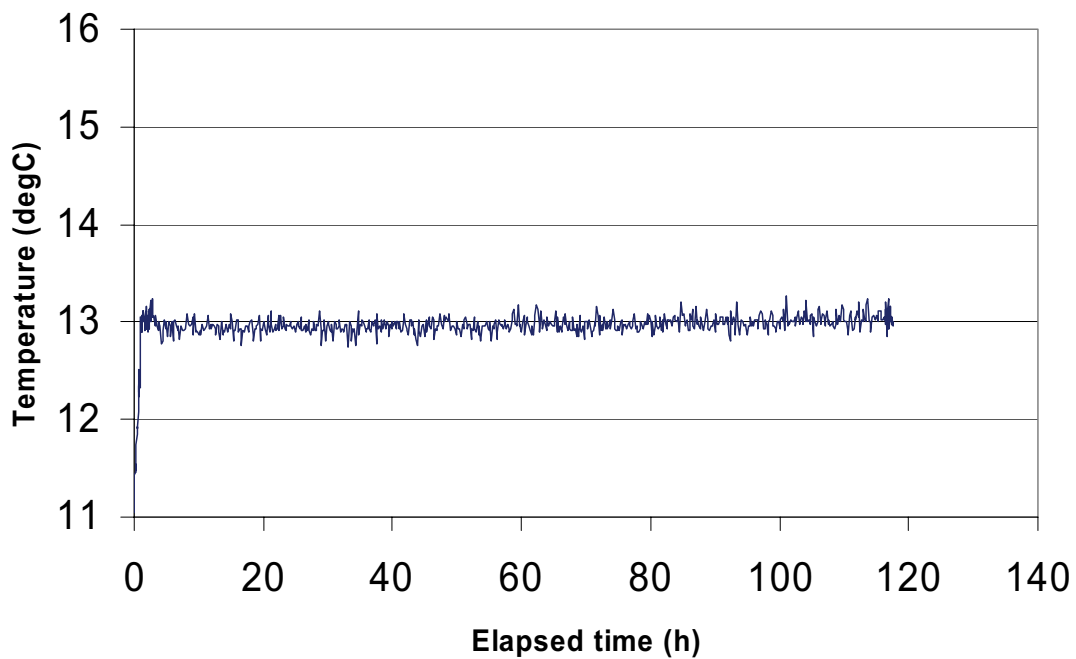
KFM08A 685.5 - 688.5 m



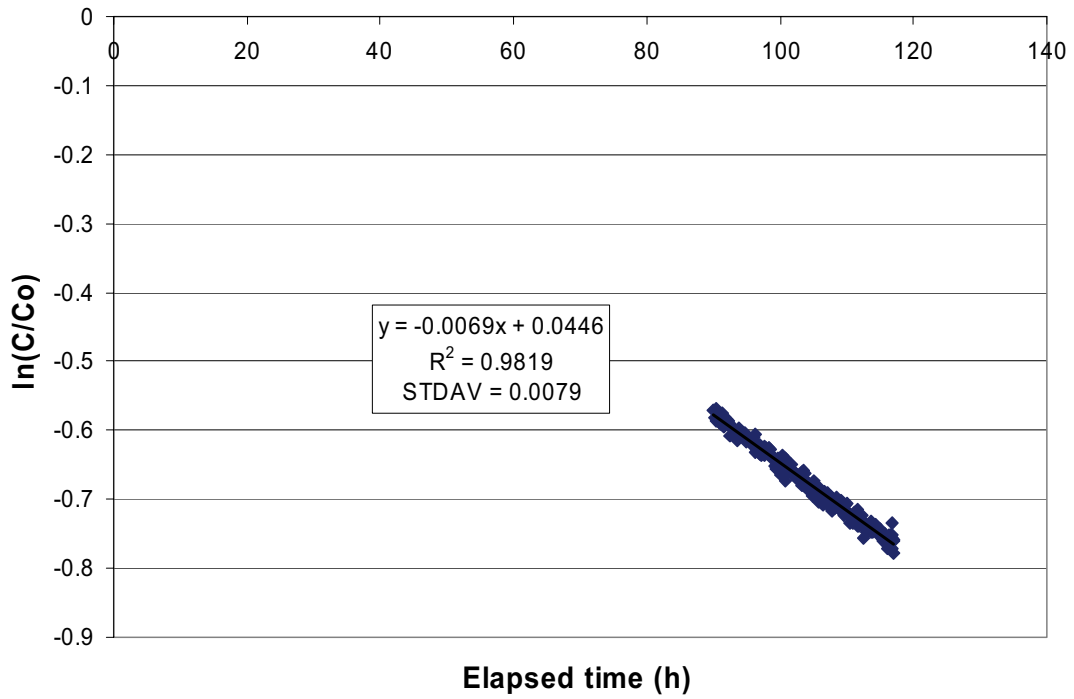
KFM08A 685.5 - 688.5 m



KFM08A 685.5 - 688.5 m



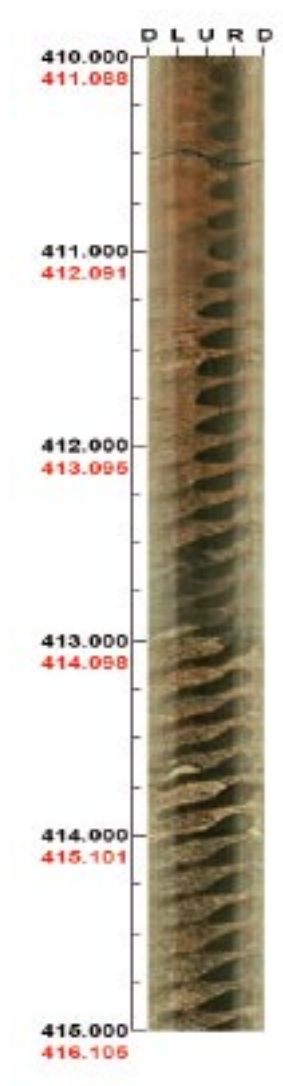
KFM08A 685.5 - 688.5 m



Part of dilution curve	V (ml)	$\ln(C/Co)/t$	Q (ml/h)	Q (ml/min)	Q (m ³ /s)	R-2value
90–117	2,200	-0.0069	15.18	0.253	4.22E-09	0.9819
Part of dilution curve	K (m/s)	Q (m ³ /s)	A (m ²)	v (m/s)	I	
35–75	4.70E-07	4.22E-09	0.4620	9.13E-09	0.019	

BIPS logging KFM08A

Depth range: 410.000 – 415.000 m



Black number = Record depth
Red number = Adjust depth

Azimuth: 319

Scale: 1/25

Inclination: - 60

Aspected ratio: 175 %